Deep Learning-Optimized Monocular Navigation for Autonomous Rendezvous and Proximity Maneuvers in Small Satellite Missions

IAC–24–D3.2B

BEYOND EARTH: A MULTIDISCIPLINARY APPROACH TO DEVELOPING SUSTAINABLE LUNAR OUTPOSTS WITH THE MOSS PROJECT

Carlo Giovanni Ferro[a*], Marco Agozzino[b], Karim Almatari[c], Sara Fesa[d], Michele Marrone[e], Luca Pasqualin[f], Armando Pastore[g], Jenna Tawfik Hussein[h], Alessandro Aimasso[i], Stefano Valvano[j], Valentina Sumini[k], Daniele Florenzano[l], Roberto Torre[m], Andrea Emanuele Maria Casini[n], Matteo Bertone[o], Paolo Maggiore[p]

[a] *Politecnico di Torino, Italy, carlo.ferro@polito.it*
[b] *Politecnico di Milano, Italy, marco.agozzino@asp-poli.it*
[c] *Politecnico di Milano, Italy, karimtharwat.almatari@asp-poli.it*
[d] *Politecnico di Milano, Italy, sara.fesa@asp-poli.it*
[e] *Politecnico di Milano, Italy, michele.marrone@asp-poli.it*
[f] *Politecnico di Torino, Italy, s308954@studenti.polito.it*
[g] *Politecnico di Torino, Italy, s308219@studenti.polito.it*
[h] *Politecnico di Milano, Italy, s314264@studenti.polito.it*
[i] *Politecnico di Torino, Italy, alessandro.aimasso@polito.it*
[j] *University of Derby, United Kingdom, s.valvano@derby.ac.uk*
[k] *Politecnico di Milano, Italy, valentina.sumini@polimi.it*
[l] *Politecnico di Milano, Italy, daniele.florenzano@mail.polimi.it*
[m] *European Space Agency (ESA/EAC), Germany, roberto.torre@esa.int*
[n] *German Aerospace Center (DLR), Germany, andrea.casini@dlr.de*
[o] *Politecnico di Torino, Italy, matteo.bertone@polito.it*
[p] *Politecnico di Torino, Italy, paolo.maggiore@polito.it*
[*] *Corresponding author*

Abstract

The MOSS Project, developed by students from Alta Scuola Politecnica, represents a groundbreaking multidisciplinary research initiative aimed at sketching an advanced moon outpost concept. Central to this endeavour is the emphasis on minimizing Earth's dependence through the innovative use of In-Situ Resource Utilization (ISRU), particularly focusing on the comprehensive utilization of lunar regolith. This project brings together aerospace and materials engineers, interior designers and architects to delve into the potential of lunar materials, developing an infrastructure that is sustainable, resilient, and scalable for satellite colonization. The research has yielded a technological roadmap highlighting processes that leverage ISRU without resorting to energy-intensive techniques, thereby filling a significant gap in the current literature regarding lunar logistical structures and spaceport manufacturing and operations. The team conducted an extensive geomorphological survey of the selected site and performed an in-depth material analysis of the lunar regolith to assess its integration with smart technologies, aiming to enhance the Technology Readiness Level (TRL) of ISRU techniques. This comprehensive approach has led to the architectural conceptualization of the moon infrastructure, encompassing self-locking landing pads, shielding walls and protective regolith shells designed to safeguard against radiation. By advancing these innovative methodologies and architectural designs, the MOSS Project aims to establish a blueprint and set criteria for future spaceports beyond Earth, thereby significantly contributing to the field of aerospace engineering and the broader quest for sustainable human presence on the Moon.

1. Introduction

Moon Outpost Smart Structures (MOSS) is a multidisciplinary exploration into the construction of advanced structures on the lunar surface. The emphasis is on minimizing resources sent from Earth through the innovative use of in-situ resource utilization (ISRU), particularly focusing on the comprehensive utilization of lunar regolith. Drawing on experience from aerospace and materials engineers, interior designers and architects the MOSS investigated the potential of lunar materials, developing an infrastructure that is sustainable, resilient, and scalable through time. The research has yielded a technological road map highlighting processes that leverage ISRU without resorting to energy-intensive techniques, thereby filling a significant gap in the current literature regarding lunar logistical structures and spaceport manufacturing

and operations. The team conducted an extensive geo-morphological survey of the selected site while performing in-depth material analysis of the lunar regolith to assess its integration with smart technologies, for brick production, aiming to enhance the technology readiness level (TRL) of ISRU techniques.

As the solutions are developed for an extremely harsh conditions, the project has two parallel potential applications: construction on the Moon's surface and in extreme Earth environments. In particular, the solutions can be utilized in territories of extreme temperature, humidity, altitudes and radiation. Furthermore, the simple assembly and disassembly of these structures make them effective for temporary situations, tackling global issues such as natural disasters, the refugee crisis. This offers a potential short-term business model to provide an alternative to the current disaster relief structural systems of tents or container homes.

Lastly, it is important to emphasize that the MOSS team aims to present a comprehensive framework for a lunar outpost. Therefore, assessing the technology's maturity level is complex, as it involves evaluating an entire system rather than a single product. Nevertheless, a concept has been already formulated and testing of the individual components is already underway as a full-scale replica of the lunar environment (LUNA) is being constructed in Cologne by ESA and DLR.

2. State of the art

The Moon, our celestial neighbor, has long captivated human imagination. Its enigmatic glow, its mysterious dark side, and its role in ancient mythologies have inspired countless tales and dreams. Yet, beyond its romantic allure, the Moon holds immense scientific and strategic value. While humanity has not been on the Moon since the Apollo missions of the 20th century, the recent resurgence of interest in lunar exploration has highlighted its potential as a hub for future Mars missions and a crucial step in human scientific advancement.
However, establishing lunar habitats presents significant challenges due to the Moon's harsh environment, the logistical complexities of transporting materials from Earth, and the long-term sustainability requirements. For this reason, a literature overview about structural concepts thought specifically for lunar settlements will be carried out hereafter. Since the project also focuses on the energy budget required to build the structural units and to run the entire outpost, a review of nuclear reactor plant designs for space application will be presented as well. Nuclear energy is identified as the main source of energy through a preliminary analysis indeed, as described later in the paper.

2.1 Lunar structures review

Early designs for lunar outposts primarily focused on prefabricated modules (Type 1 structures) manufactured using the large industrial base and assembly lines available on Earth, transported intact using the present logistical infrastructure. These modules were meticulously engineered to fit within launch vehicle constraints contemporarily available, often adopting cylindrical shapes to maximize cargo space. While this approach offered a familiar and relatively straightforward solution, it faced a significant drawback: the exorbitant cost per square meter. The transportation of fully assembled modules to the Moon, coupled with the limited cargo capacity of launch vehicles, resulted in a high price tag for each unit of habitable space. This typology also fails to consider the scenario of expanding settlements and growing needs, relying on decisions and assumptions made in earlier design phases, sometimes many years before delivery. The only examples of space architecture realized are almost all exclusively of this nature, including the ISS and Apollo Lunar Module [1, 2].
Inflatable structures (Type 2 structures) offer a promising alternative due to their lightweight and compact nature, adaptability, rapid deployment capabilities, potential for radiation shielding, and cost-effectiveness compared to traditional construction methods. The inflatable nature of this structure family means that the surface is made of air-filled double membranes as opposed to the heavier metals employed in the aforementioned prefabricated modules. These positives allow for a reduction in the cost of transport per cubic meter while maintaining some form of design oversight from those managing from Earth. On the other hand, while they may face challenges such as puncture vulnerability and pressure maintenance, ongoing research and technological advancements are addressing these issues, making inflatable structures a viable option for future lunar exploration. Type 2 structures have undergone some real-world texting with only BEAM (Bigelow Expandable Activity Module) being an example implemented.
The third alternative, In-situ resource utilization (ISRU) techniques, which involve utilizing lunar materials for construction and other purposes (Type 3 structures), hold the promise of reducing reliance on Earth-based resources and enabling more sustainable and self-sufficient lunar outposts. By leveraging lunar materials, it may be possible to construct habitats that are more resilient to the harsh lunar environment and require less frequent resupply missions. Type 3 structures could pass the creative freedom to the inhabitants themselves, shortening the

feedback loop and speeding critical decision-making, especially in harsh and foreign environments such as the lunar surface. Another outcome would be the increased speeds of the dynamics of innovation as any designs are freed from the constraints and standards imposed in Types 1 and 2. Literature review shows a clear majority of designs and papers regarding the exploration of this method, owing to the advantages described previously and the opportunities it inherently entails such as Project Olympus by NASA and the Moon Village by ESA [1].

Within Type 3 structures, there exist many sub-proposals as diverse as the history of construction itself. The composition of lunar regolith resembles clay and cement specimens on Earth as the closest equivalent, owing to their chemical composition. Compression-based construction methods are the best way forward for this composition by correlation. Many solutions exist to reach this goal, including 3D printing, block making, baking and sintering. Within each, a different road-map and timescale are required.

The vast landscape of ISRU techniques can be more easily understood by separating building methods into two main classes according to the strategy applied to form a solid structural material from what is essentially a loose powder. A first approach involves the thermal processing of the regolith powder in order to either induce melting or local surface diffusion between the grains and to form a solid material. The second paradigm proposes the use of a binder, either organic or inorganic to form the structural elements. In both cases, 3D printing is a widely applied concept and the most common strategies involve the fabrication of empty shells that will be then filled with loose regolith, providing radiation shielding and protection from micrometeorite impact. Both approaches have strong points and weaknesses as sintering is indeed energy intensive but also the use of a binder requires large loads to be sent from earth. This complex discussion will be brought forward in the section dedicated to our solution. Furthermore, in this work, a slightly different perspective is adopted: energy consumption and cost are not the only metric on which a building technique should be judged but reliability must also be included in the evaluation. Thus, the most promising ISRU technique will also be the simplest.

As presented in this paper, the MOSS project aims to establish a case study for a lunar outpost based on the third type of structure: constructing a settlement using tiles composed of a lunar regolith and polymer mixture. By prioritizing in-situ resource utilization, the project seeks to minimize the materials required from Earth. This approach limits the necessary Earth-sourced materials to the tools needed for tile production, which would be sent to the Moon on a one-time basis, as well as the polymer. Furthermore, this approach also limits the energy budget. It is indeed true that there is no consensus on the energy source to be adopted in a lunar settlement but the relevant literature is in agreement that the minimization of energy consumption is a key goal, as to reduce fmission complexity.

3. Conquering the Moon: from cartography to a lunar outpost

Lunar Cartography and Selenography (the study of the surface and physical features of the Moon [3]) can provide valuable tools to understand the context and the palimpsest that it is comprised of. The Moon is primarily consisting of three major macro-regions or landforms: mountain-chain highlands, large flat plain maria and Impact craters. The photomosaic in Fig. 1 showcases the distribution and specific names of the landforms. The data was acquired by NASA's long-running Lunar Reconnaissance Orbiter (LRO) spacecraft, a $500 million project [4]. The area of interest lies on the South Pole of the Moon (cartographically between 70 and 90 degrees south of the parallel).

The area is rich in impact craters from meteors millions of years ago, creating permanently shaded areas rumored to host ice. Ice is a valuable resource and crucial for energy production and water harvesting.

Zooming in further, the features of the south pole can be begun to be appreciated. Nasa's Moon Mineralogy Mapper (M3) in 2018 has scanned and found direct evidence of ice embedded in the permanent shadow regions of craters.

The map below showcases the density of ice in relation to the geography, with the highest concentration appearing to be in the Shackleton Crater, the closest to the geographical South pole at 89 °. It is also no surprise that Shackleton is also the proposed landing site for many of the lunar missions in the next decades.

3.0.1 The Moon's geology

The area is classified as an Eratosthenian Crater, which is a circular crater characterized by sharp rim crests and containing parts of eject along the circumference. The composition and morphology of the inside are based on the primary impact event that has caused the landform to exist. Outside the Shackleton crater, the region is defined as a Pre-Nectarian Basin: "subdued, eroded mountain rings, rims, walls, and inner ring materials. The morphology is probably caused by erosionally degraded impact-related structures and ejecta materials" [5]. This is quite evident from the maps reported in Fig. 5.

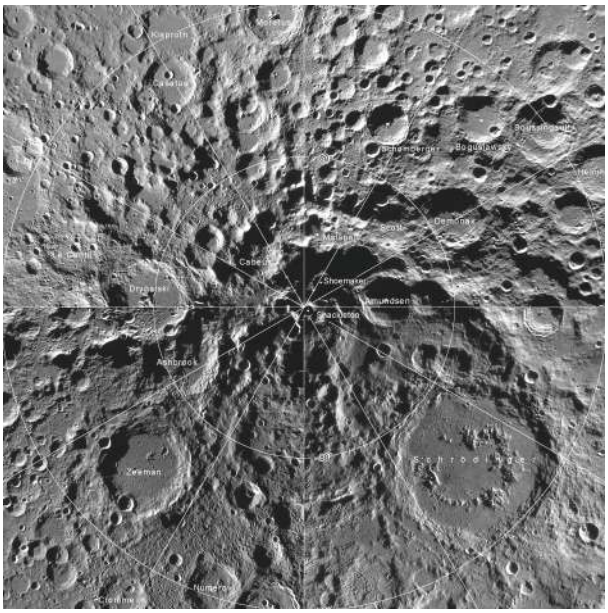

Fig. 1. Image Map of the Lunar South Pole [6].

- **Relief and Surface Marking**: The map created by data collected by the Lunar Orbiter IV spacecraft showcases the difference in height across the pole. It can be seen that the craters are in fact of massive scale compared to Earth counterparts. It is noteworthy the plains to the "East" of the Shackleton Crater, suggest a flat area capable of supporting an expanding base that is also next to the ice-rich craters.
- **Polar Chart**: The Lunar Polar chart (LM-3) was an attempt to create the most detailed map of the Moon for NASA and the US Air-force towards the end of the 20th century. The key was to name and catalog all the features on the Moon and acts as an important reference document.
- **Topography**: The southern pole is an area of extreme differences in altitude. From the bottom of the crater to the top of the rim is a difference of 4 kilometers. This mountainous terrain should be taken into account in the design proposal.

3.1 Methodology

3.1.1 Spaceports: current examples and proposals

Terrestrial spaceports Spaceports on Earth, such as Spaceport America and Spaceport Japan (Fig. 5), provide a framework for future equivalent on the Moon. Spaceport America is the world's first purpose-built commercial spaceport, designed to cater to vertical and horizontal space vehicles. It is located in Sierra County, New Mexico, USA, owned by Virgin Galactic and features a giant shell structure with a sinusoidal main facade and an arc back elevation [12].

The spaceport has been open since 2011 and has been operational ever since [13].

Spaceport Japan, an unrealized project in the heart of the metropolitan city of Tokyo, aims to be Asia's first spaceport.

The structure consists of a short cylindrical structure with a sinusoidal roof as a base hub, branching arms for ingress and egress of space vehicles.

Spaceport America works by its continued operation and realization, with its simplicity in system design allowing for effective carrying out of functions and the concentration of facilities.

The architecture attempts to be built into an artificial hill, showcasing consideration towards topology in an otherwise flat context. Spaceport Japan offers an optimistic example of the potential of the typology, envisioning more gateways and infrastructure to connect it with the rest of Tokyo.

However, Spaceport America has not been tested for large vertical spacecraft ingress and egress, lacks capability for other functions besides logistics and storage, and does not offer insight into expansion in case of increased demand.

Spaceport Japan's ambitious design could have a more efficient system for main highways going in and out of the structure, but there are still questions about the facilitation of large vertical spacecraft.

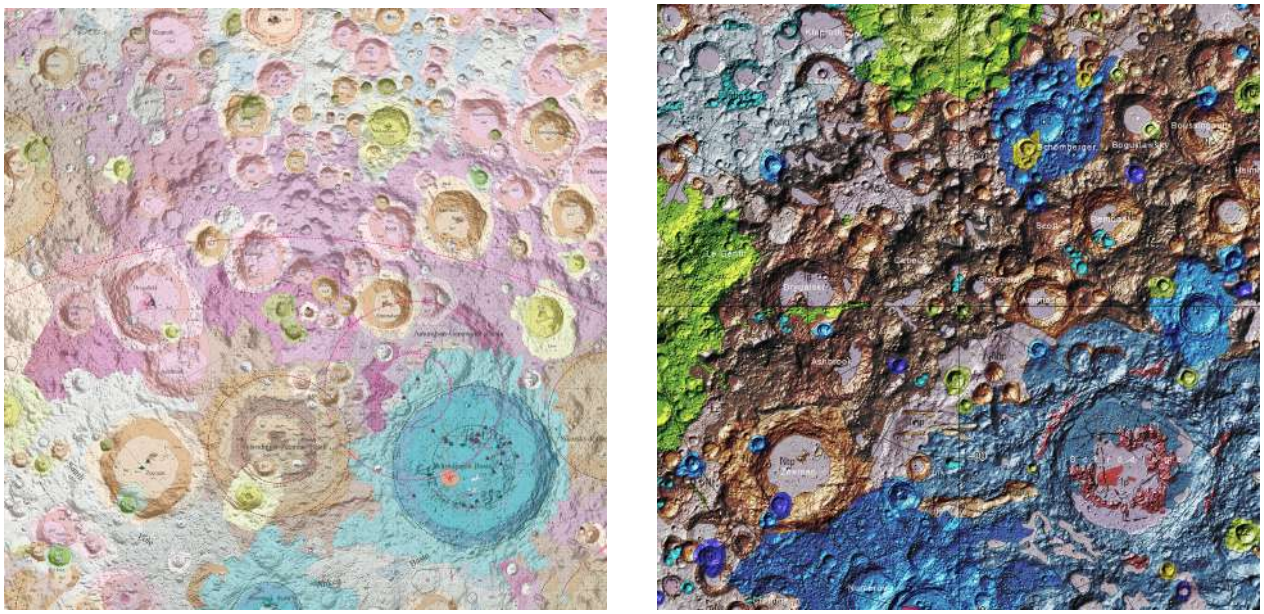

(a) (b)

Fig. 2. (a) Geological map by CNSA (China National Space Authority) [7]. (b) Unified Geologic Map of the Moon [5].

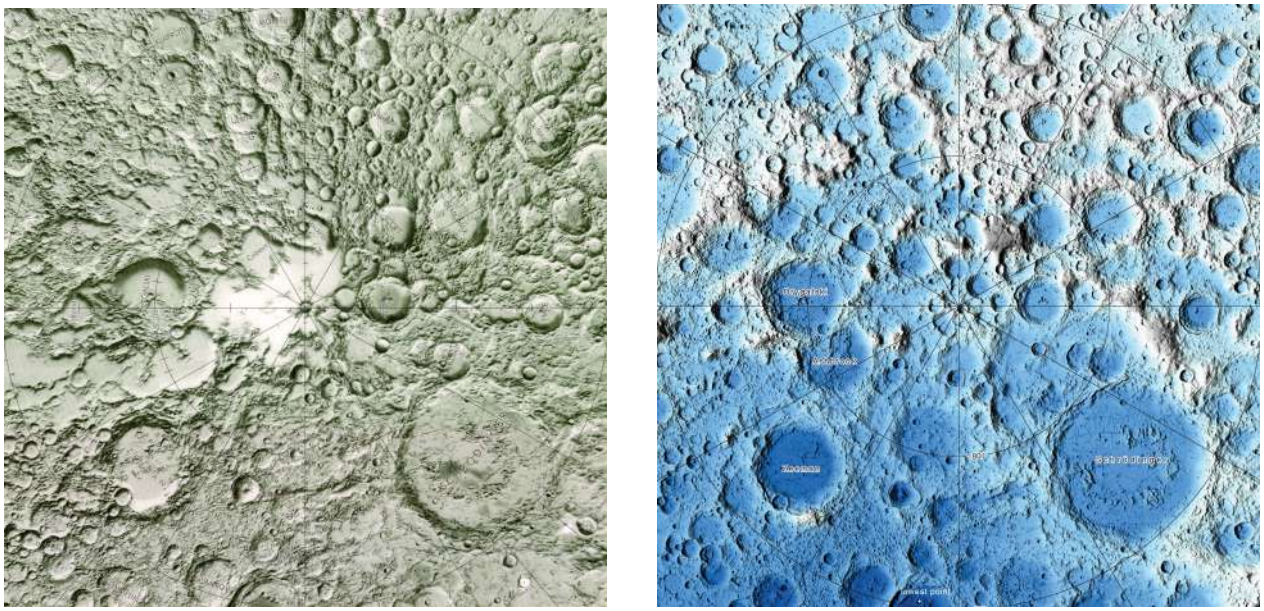

(a) (b)

Fig. 3. (c) Shaded Relief Map of the Lunar Polar Regions [8]. (d) South Pole Topographic Map [9].

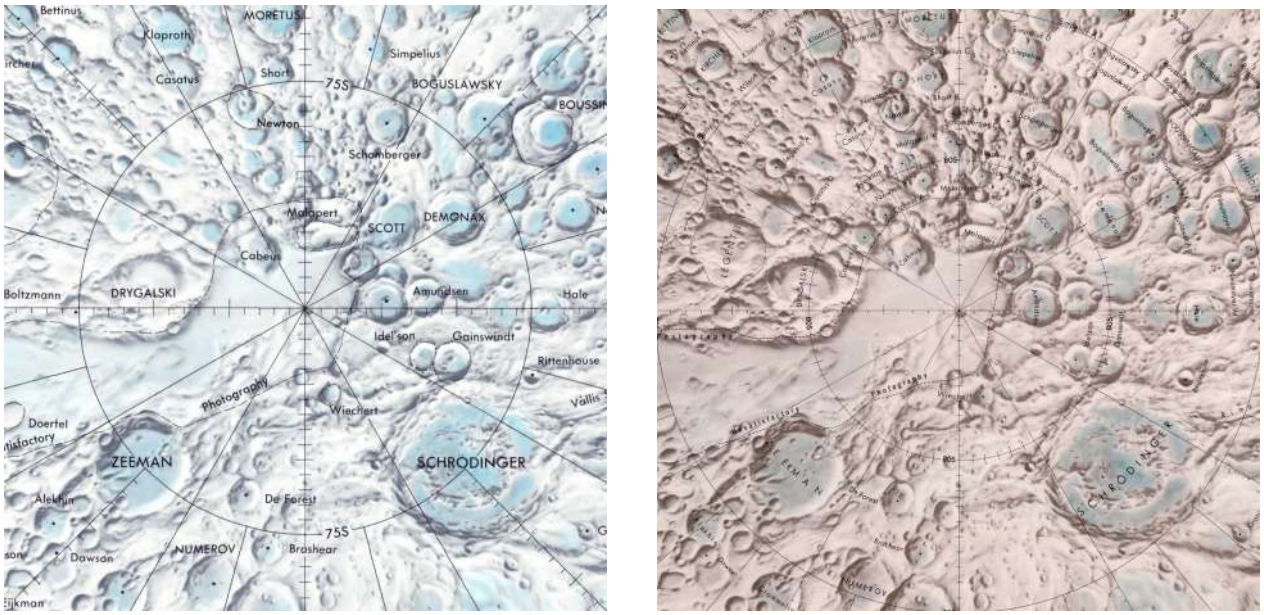

(a) (b)

Fig. 4. (e) Lunar Chart 1979 version [10]. (f) Lunar Polar Chart [11].

Both examples offer the closest insight into the direction of spaceports on Earth and on other celestial objects.
They offer proof that such structures could exist, and their renders and technical documents are a guide to the design process and aspects to pay attention to. Most of the functions are beyond the scope of this project but appreciative of ambition.

Airports This section discusses the design of airports in different contexts, including extreme environments and metropolitan world capitals. The Red Sea International Airport (Fig. 6), designed by Foster and Partners, is a sustainable and echo-friendly terminal on Saudi Arabia's west coast [15]. The Amaala airport, located on Saudi Arabia's northwestern coast, morphs to mimic a desert mirage, similar to the Red Sea airport [16]. The Charles De Gaulle Airport in Paris, one of the busiest European airports, is a prime example of program organization [17]. The Red Sea airport is designed to run on 100% renewable energy and minimize embodied carbon through design development. Its paradoxical smooth edges are inspired by desert dunes, while the Amaala airport features climate-controlled hangars and ground transfer service. The Charles De Gaulle airport has several small operating sub-unit airports connected through an underground tunnel to a main airport, acting as a landscape.
The Red Sea Airport morphology mimics the desert dunes and the choice of color allows it to blend within its environment. The contractual scope includes aeronautical navigational aids, air-side utilities, and aerodrome grounding lighting helipads. The shape of the roof cantilevers to provide shade to passengers. Both examples based on the harsh Saudi heat provide a reference for protection from exterior harsh conditions that can apply to lunar contexts, whereas the example of Charles De Gaulle could provide a blueprint for the spatial organization of the program around a central command center that acts as a nucleus for the project.

Movies Due to the extreme novelty of the typology proposed, it is important to also appeal to the state-of-the-art spaceports in movies and the creative industry, which are now at the forefront of the contemporary debate. Two have been selected for debate, selected specifically for their interpretation of the topic. The first is Clavius Base from the 1968 film "2001: A Space Odyssey", which features a space port that is built underground to protect from micrometeorites and solar radiation, with the infrastructure separated from the rest of the base proper [18]. The second example is Rhea Base from the 2016 film "Independence Day: Resurgence" (Fig. 6). This military base on the Moon features a spaceport for fixed-wing and rocket spacecraft as an offshoot of the central site, favoring instead transportation via lunar rovers and EVA [19].
Clavius Base benefits from building and utilizing the crater surface of the Moon, allowing the use of the benefits

(a) (b)

Fig. 5. (a) Spaceport Japan Visualization [13]. (b) Spaceport America drone shot [14].

(a) (b)

Fig. 6. Front (a) and top (b) view if the Red Sea International Airport [15].

provided in terms of a starting foundation for construction, the dynamic dome allows for further protection and limits the launchpad exposure only when necessary. Rhea base works in the movie as it anticipates a less mature stage of the project as well as expecting spacecraft to be more like the space shuttle than current rocket models, with a greater use for the runway than the launchpad. This reduces problems such as the effect of extreme heat on the infrastructure coming from rockets and logistic storage.
The spaceport specifically, is also over-engineered and relies on systems requiring a lot of power for a result that could probably be achieved in simpler methods. Due to the lack of air resistance on the Moon and other drag factors, the movie leaves a lot of questions unanswered. The disposition of the spaceport to the base has proven beneficial in both cases, reducing potential accidents, and separating potential issues from each other instead of compounding them.

Architectural competitions/proposals Examples from the architectural realm provide analysis by conceptualizing proposals. The example of Project Olympus. created by Bjarke Ingles and SEArch+ studio illustrates the potential of robotic construction using 3D printing [21]. Imagining an entire colony on the Moon, this state-of-the-art concerns itself with the landing pads. SpaceX has produced conceptual renders, displaying the urban planning approach with energy and logistics (Fig. 8) [22]. ISRU was addressed in the Vision of Lunar Settlements by SOM and the Mars Habitat Competition by Foster and Partners, with attention to modularity as a powerful tool in colony expansion [23]. Project Olympus is an effective solution as it limits the amount of resources transported from Earth creating 3d printed infrastructures using materials available on the lunar surface, a sustainable solution. The design of the landing pads recommends building a regolith ring controlling debris arising from the spacecraft engines, which disturbs the instruments on the Moon, compromising mission success. Space X suggests the use of large vertical spacecraft to conduct logistics which is more efficient. As for the role of 3D printing and ISRU, the two competition entries are a controlled approach which are studied to apply to the design.
The documentation for Project Olympus lacks technical details to judge for proper scrutiny, therefore is heavily dependent on the graphic material. Space X receives more criticism as the base does not have a land pad nor a solution to offload resources. The project by SOM either requires a hybrid, type 1 structure, or giant printing robots which require sufficient energy and resources, beyond the technological capability of the industry. Our project aims to maximize use of in-situ resources for building material, therefore SOM's proposal would be difficult to replicate using building systems created by regolith blocks. With attention to the construction time, modular structures allow faster assembly and less energy.
Project Olympus contains atmospheric pressure utilizing it for protection from cosmic and solar radiation. The design for landing pads could be applied to the project due to its feasibility and lower energy requirements. Space X's renders emphasis the need for distribution of services. ISRU is the primary technique in construction, providing insight into the application of this technology. The master-planning of project Olympus illustrates the connections between the main logistics hub and the landing pad replicating a road-like structure to implement a mobility network using rovers, minimizing distances walked by astronauts.

3.2 Execution and results

The following map (Fig. 9) illustrates the topographic plan of the lunar surface, at a scale 1:100,000 dividing the site in an equal grid of 1km by 1km. Highlighted are the different potential areas for locating our project as well as the spot elevation and contour lines, where each line represents a 50m level difference. This is imperative to our early design phase as it gives an overall understanding of the topography and terrain formation, essential to take into consideration when selecting the potential site for our project.

3.2.1 Program Distribution

Figure 10 contains a scheme of the progress road-map that has been envisioned for this mission. **Phase 1: Outpost**
Population: None Permanent
In the first phase, the main goal is to achieve essential and minimum function capacity, beginning by selecting the area with least risk and highest potential. Phase 1 strives to satisfy the demands of the ISRU and printer to execute the design coupled with a receiving point for cargo from Earth. Prefabricated units may be required should human supervision be necessary.
Phase 2: Lunar Base
Population: 4-6 on Rotational basis
In this phase, the mission aims to be as self-sufficient as possible, yet still allowing for periodic replenishment from Earth. Project MOSS now acts as an outpost with similar capabilities as an off-grid bases. The project will still be logistical and research in nature. The entire settlement will be the spaceport and its infrastructure. The focus will be on this phase of the project

(a) (b)

Fig. 7. (a) Movie still of Rhea Base from"Independence Day: Resurgence" [19]. (b) Rhea Base Concept Art [20].

(a) (b)

Fig. 8. Project Olympus by BIG and SEArch+ [21].

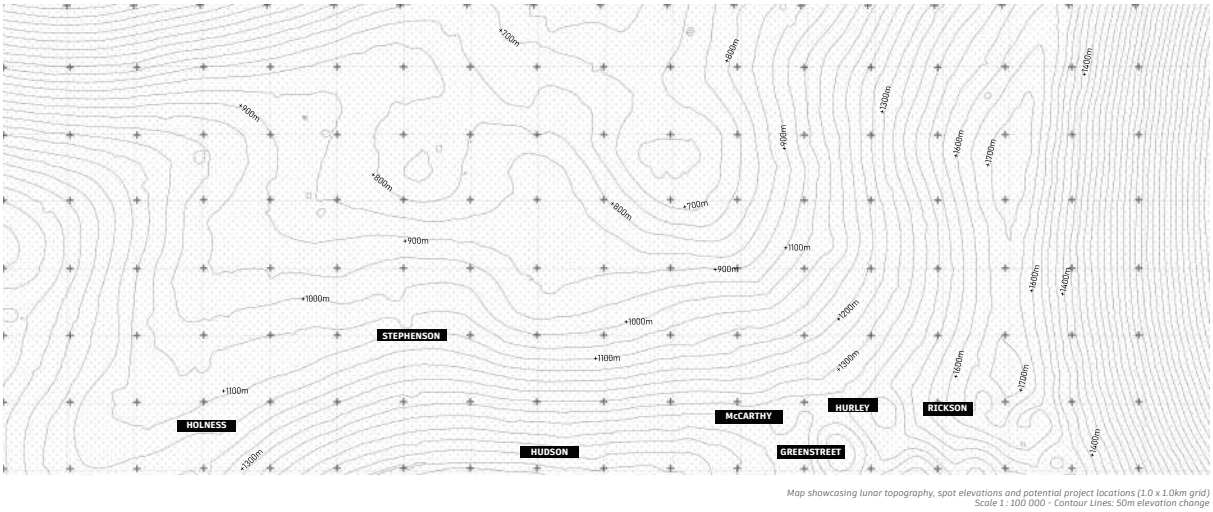

Fig. 9. Map showcasing lunar topography, spot elevations and potential project locations (1.0 x 1.0km grid).

Phase 3: Lunar Colony *Population: 50+* A lunar colony begins to be self-supporting with supply above demand. Resilience allows for a net-positive settlement producing goods and services. Beyond this stage, the project's scope extends into the realm of science fiction and is not addressed within the current framework.

3.2.2 Function dimensions

Given the unique nature of the project's brief, finding comparative precedents and case studies to determine the required dimensions can be challenging. The plan of action was therefore to split up the final building into its constituent parts and find comparative estimations for those instead before totaling them up all together again.

The following tables showcases a collection of data points taken from literature reviews, mission requirements and manuals with the recommended space for each function calculated based on the brief thereafter, including relative sizes and alternative systems of supplementary infrastructure and/or technologies.

3.2.3 Masterplan

The footprint plan provides a detailed visualization of the project's placement once it is implemented onto the designated site.

This schematic outline in Fig. 11 illustrates how our project is strategically embedded within the unique topography of the lunar surface.

By carefully analyzing the terrain, we have ensured that the flat regions are utilized optimally to facilitate adequate connections through a well-organized network of roads. These roads are designed to seamlessly connect various key components of the project.

The launch pads are strategically positioned with adjacent back-up landing pads, meticulously respecting the minimum required distances between each pad. This careful planning ensures safety and efficiency in operations. The network of roads links these launch and landing pads directly to the main spaceport, creating a central hub for transportation and logistics. Additionally, the layout includes connections to the essential infrastructure, such as the nuclear and solar power plants. The placement of these facilities has been thoughtfully considered to optimize energy distribution while maintaining the integrity of the lunar environment.

3.2.4 Design of the structure

The design choices for the lunar landing pad (LLP) were made following a myriad of technical and geometrical challenges.

Primarily, the radius (80m-100m) was chosen following the latest technical manuals for vertical spacecraft landing pads on Earth. The wall height followed the need to make sure all ejecta and lunar dust following the takeoff and landing of space vehicles to be contained. For the

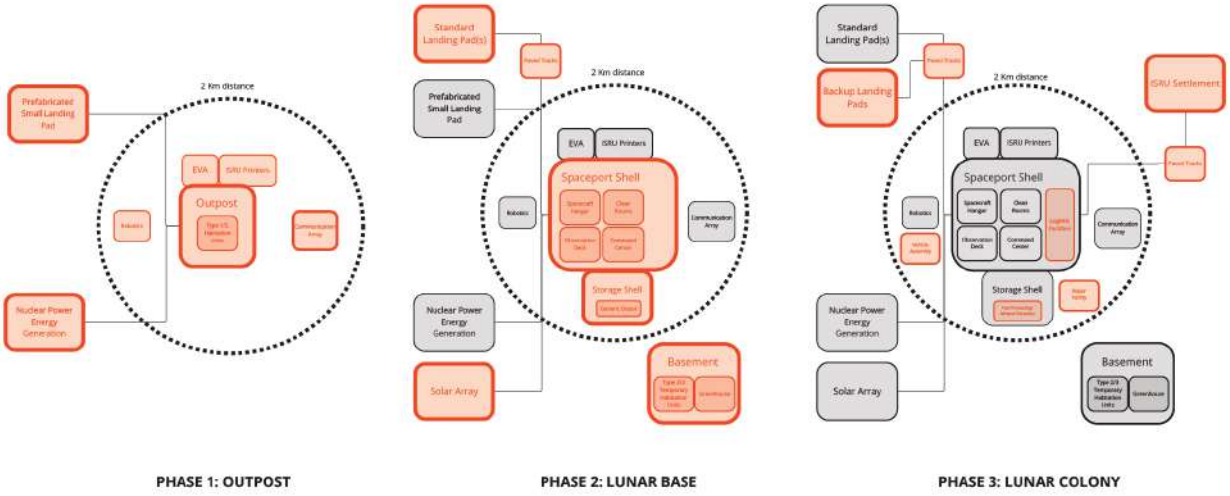

Fig. 10. Compositional diagram illustrating the design of the distribution program divided into three distinct phases.

Communication Array		
Reference Values		
Lunar Communication Satellite	(Schmid et al., 1968) [24]	1.60 m diameter
Internalized Function	(Burke & Howard, 2022) [25]	2.10 sqm
Teleoperation and Crew Communication	(Stromgren et al., 2020) [26]	1.70 sqm
Project M.O.S.S. Allocated Area		**2.10 sqm (external)**
Solar Array		
Reference Values		
Energy Demand as per Mission (Constant)	(Wertz & Larson, 1999) [27]	29.4 KWe
Energy Demand as per Mission (Construction)	(ASP, 2024)	35.6 KWe
Available Solar Intensity	(Colozza et al., 2010) [28]	1301 W/m^2
Solar Panel Efficiency on the Moon	(Jingsun, 2023) [29]	25%
Project M.O.S.S. Allocated Area		**200 sqm**
Nuclear Power Reactor		
Reference Values		
Energy Demand Check	(Molteni, 2022) [30]	65 KWe
NASA Kilopower Project Energy Production	(Gibson et al., 2017) [31]	10 KWe
Safety Distance (-1m offset from ground)	(ASP, 2024)	50m
NASA Kilopower size	(Palac, 2016) [32]	4.00 m diameter
Project M.O.S.S. Allocated Area		**28 sqm**
Landing Pads		
Reference Values		
ICON's Project Olympus	(ICON, 2023) [33]	75-100m diameter
SpaceX Landing Pads, Florida	(WP, 2017) [34]	86m diameter
SpaceX Backup Landing Pads	(Google Maps, 2024) [35]	43m diameter
Lunar Spaceport Concept	(Anderson et al., 2020) [36]	120m diameter
Lunar In-situ Landing/Launch Environment (LILL-E) Pad	(Burns et al., 2021) [37]	50m + 150m diameter
Number of Landing Pads Required	Mission Scenario	3+3
Project M.O.S.S. Allocated Area		**100m diameter**

EVA (Extravehicular Activity)		
Reference Values		
Lunar Roving Vehicle (LRV) a.k.a. Moon buggy	(NASA, 2016) [38]	3.00m x 2.30m
Space Exploration Vehicle	(NASA, 2010) [39]	4.50m x 4.00m
Lunar Terrain Vehicle	(GM, 2024) [40]	Of Similar Dimension
Spacecraft Hangar (Internal)		
Reference Values		
Space Shuttle (The Orbiter)	(NASA, 2023) [41]	25.00m Radius
SpaceX Dragon 2 Capsule	(SpaceX, 2024)	4 x 4 x 8.1m
Apollo Lunar Module	(Orloff, Richard, 1996) [42]	4.20m Diameter
General Depot		
Reference Values		
Food required per person per year	(Russomano, 2016) [43]	225.20 kg pp pa
Water required per person per year	(Russomano, 2016)	1427.15 kg pp pa
Oxygen required per person per year	(Russomano, 2016)	306.6 kg pp pa
Total Resource volume required per person per year	(Rahman & Rahman, 2009) [44]	$\sim 3m^3$ pp pa
Observation Deck		
Reference Values		
ISS Cupola	(ESA, 2024) [45]	2.00m diameter
TWA Flight Center Lounge by Eero Saarinen	(Metalocus, 2024)	126 sqm
Project M.O.S.S. Allocated Area		**50 sqm**
Command Centre		
Reference Values		
Lunar Base Command Centre	(Burke & Howard, 2022)	2.10 sqm

highest angled debris (15-17 degrees), a 15m tall rim with a 2m drop should prove sufficient. This is made clear in the diagram in Fig. 12

The thickness corresponds to the need for structural stability as well as blocking most of the radiation from sources on the Moon. Multiple tunnels leading into and out of the LLP, allow for separate portals for human and cargo access and to allow for contingencies. The positioning at right angles nullifies danger to both from a single dimension risk.

The LLP would come in pairs as a backup LLP would educe risk in an uncertain context. It is envisioned to have three of these pairs. Figure 13 contains a series of renders of the proposed design.

4. Design and validation of a structural element from ISRU materials

Having established a roadmap for the development of a lunar outpost, it is clear that the manufacturing of a landing pad will represent the most crucial step [46]. Thus, this infrastructure has been taken as a case study for the implementation of a structural element fabricated from ISRU materials. Key to this endeavour is the need for minimising the weight brought from Earth, imposing an interlocking design thus eliminating the need for a binder during the assembly of the pad.

In this section, a novel approach to ISRU involving the use of a polymer-regolith blend is discussed and the design of a tile is derived starting from the processing characteristics of the material. Secondly, the design is validated by simulating the impact of a fully loaded European Large Logistic Lander.

4.1 Material Properties and tile design

The lunar surface is covered by a layer of fine sand-like material that is called Regolith. Given its abundance, it is only natural that any successful ISRU building technique should employ it as the main building material.

The vast landscape of ISRU techniques can be more easily understood by separating building methods into two main classes according to the strategy applied to form a solid structural material from what is essentially a loose powder. A first approach involves the thermal processing of the regolith powder in order to either induce melting or local surface diffusion between the grains and to form a solid material [47]. The second paradigm proposes the use of a binder, either organic or inorganic to form the structural elements. In both cases, 3D printing is a widely applied concept and the most common strategies involve the fabrication of empty shells that will be then

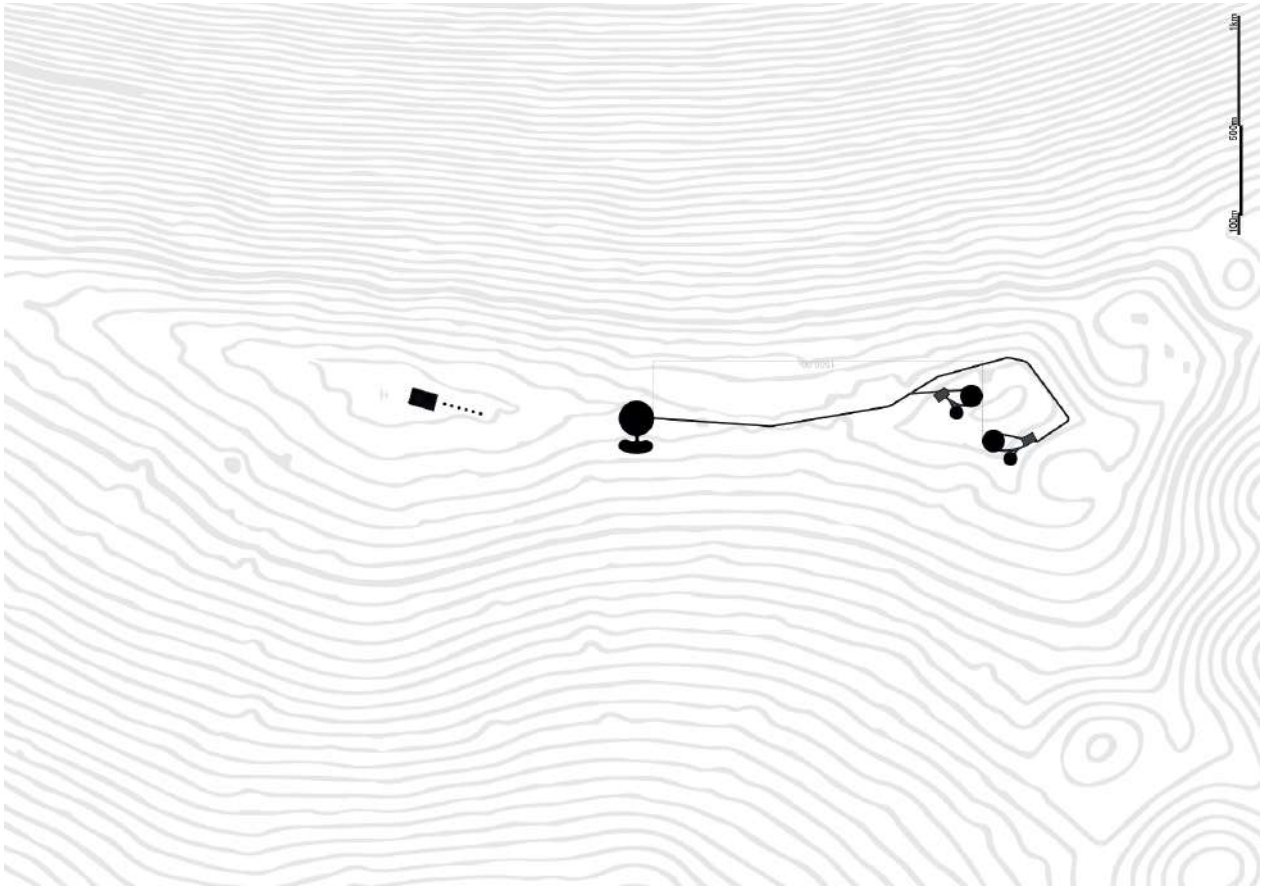

Fig. 11. Architectural map describing the Footprint Plan designed for the lunar surface.

filled with loose regolith, providing radiation shielding and protection from micrometeorite impact [48]. Both approaches have strong points and weaknesses as sintering is indeed energy intensive but also the use of a binder requires large loads to be sent from Earth.
In this work the material that has been explored consists in a blend between regolith and a thermoplastic polymer (Poly Ether-Ether Ketone, PEEK). First proposed by Torre et al., it allows to form solid elements through compaction of the blended powder in molds that are subsequently heated to induce melting of the polymer fraction [49].
It is true that part of the flexibility associated with 3D printing is lost but the streamlined process greatly reduces complexity and thus is intrinsically more reliable. Furthermore, it eliminates the need to handle a liquid binder associated with widely investigated binder jet techniques [50].
To investigate the effect of binder content and compaction pressure, a Design of Experiment (DoE) study was set up considering 12 runs, each corresponding to one of the possible combinations given by the chosen three values of binder content (5, 10 and 15 wt. %) and four values of compaction pressure (0.5, 2.5, 5, and 7.5 MPa).

The stress-strain curves reported in Fig. 14a result from flexural testing of the specimens according to ASTM standard D790-17 [51]. A brittle behavior of the material is evidenced, possibly as a consequence of the presence of voids between the regolith particles not filled by the polymer fraction. More in depth post-mortem analysis through optical or electron microscopy is needed in order to elucidate the failure mechanism of this material.
Unsurprisingly, from Fig. 14b it is evident that the binder content has a strong effect on mechanical properties that are further tuned by the compaction pressure.

Given the brittle nature of this material, a valid tile design should minimise the potential for stress intensification. The form finding process has started by considering the 2D shapes in Fig. 15a, the third option from the left has been chosen as it did not show any abrupt change in cross section or acute angles. Subsequently, this basic shape was

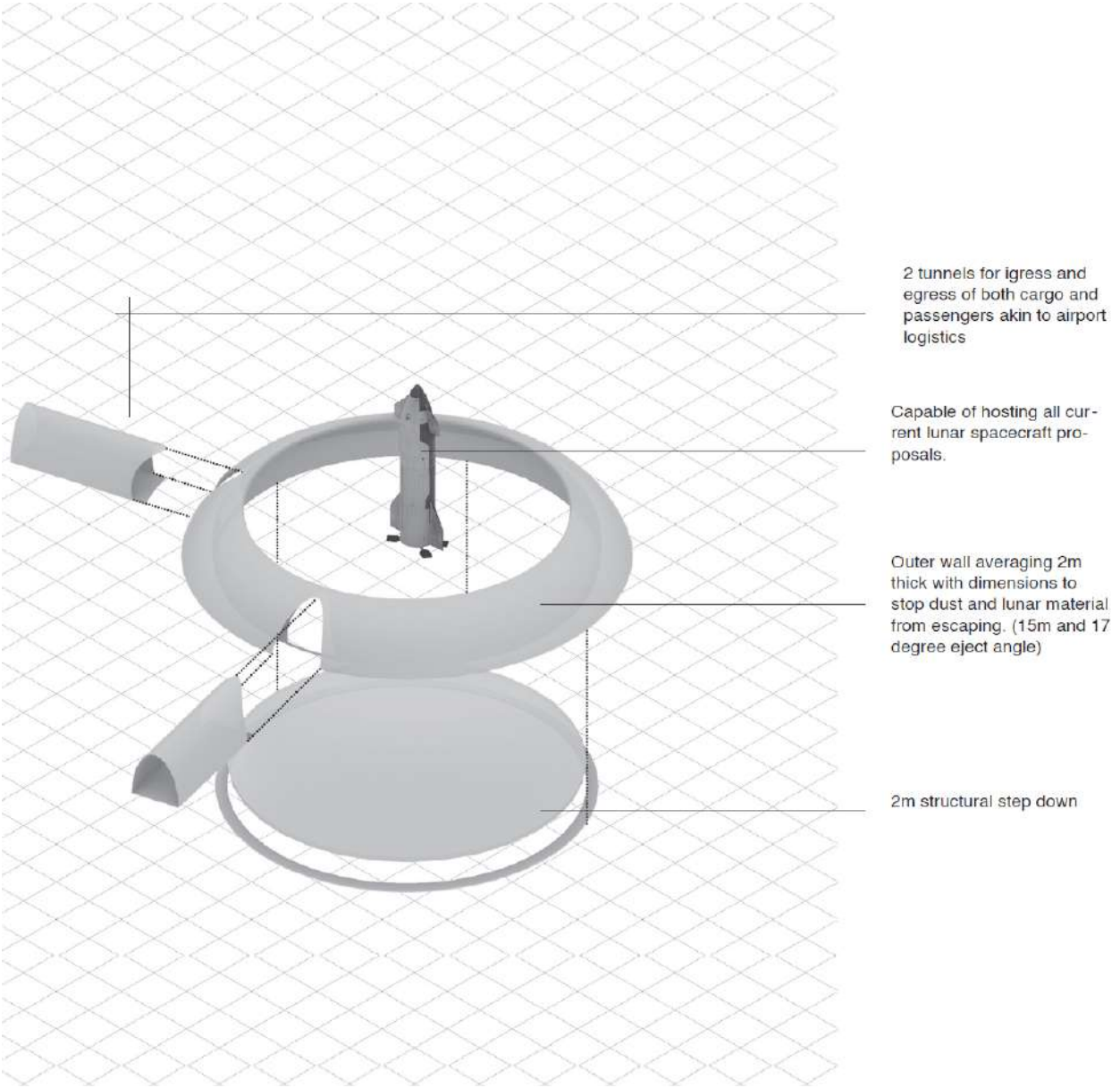

Fig. 12. Exploded Axonometric Diagram

refined into the design in Fig. 15b by adding a 5° relief on the sides to aid in extraction from the mold. Furthermore, coupling features have been added to allow for tile stacking. This allows for redundancy and ease of maintenance. Note that being the binder a thermoplastic polymer, the damaged element can be ground and easily reshaped.

4.2 Simulation setup

The following sections describe the conducted campaign of simulations that have been performed on the selected design of tiles. Specifically, in the Altair RADIOSS environment it has been possible to model and analyse, through an explicit FEM method, the structural response of the assembly of tiles, represented below in Figure 16a, of the landing of Argonaut, ESA's autonomous lunar lander [52].

From reference [52] is possible to acquire the necessary information about the lander's structure, inertia and materials. Specifically, the available data is listed below:

- Landing mass, given by the sum of the cargo platform

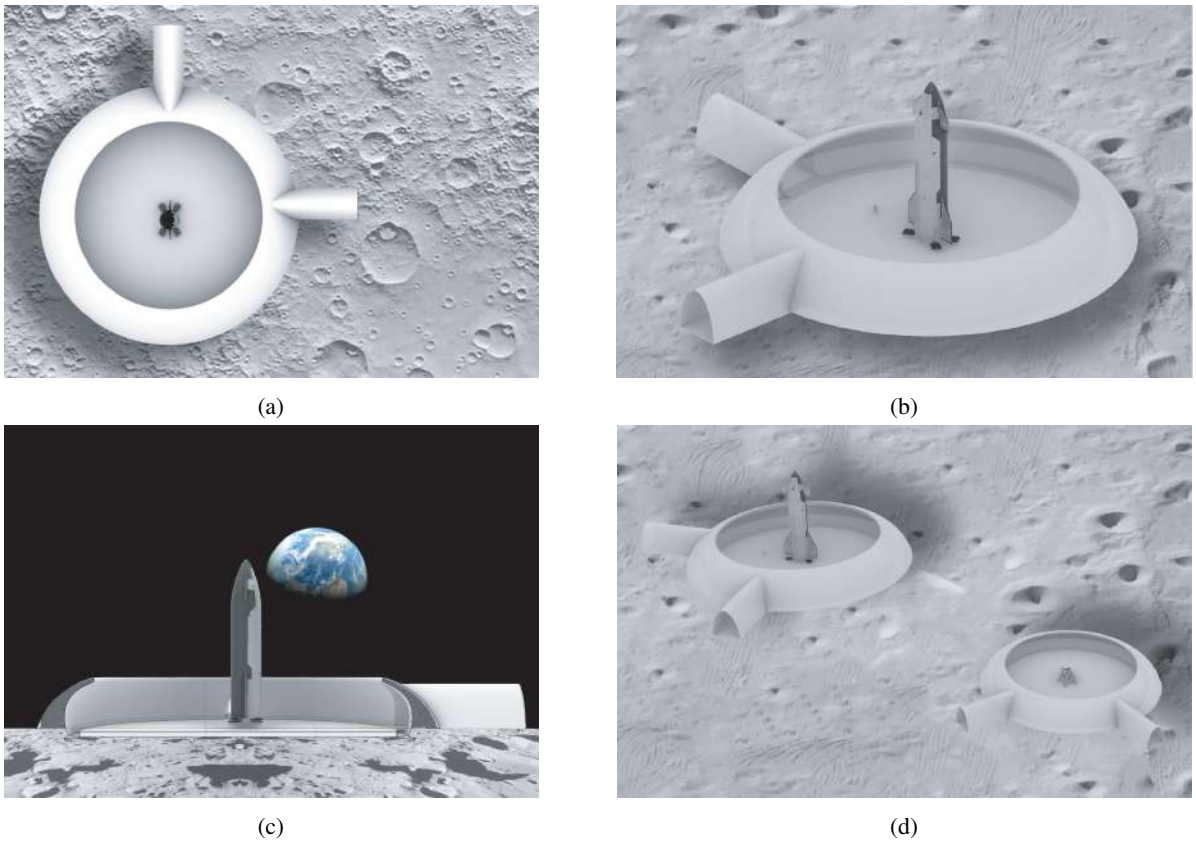

(a) (b)

(c) (d)

Fig. 13. (a) Top View of the LLP. (b) Axonometric View of the LLP. (b) Section of the structure. (c) Lunar Landing Pad with Backup Infrastructure.

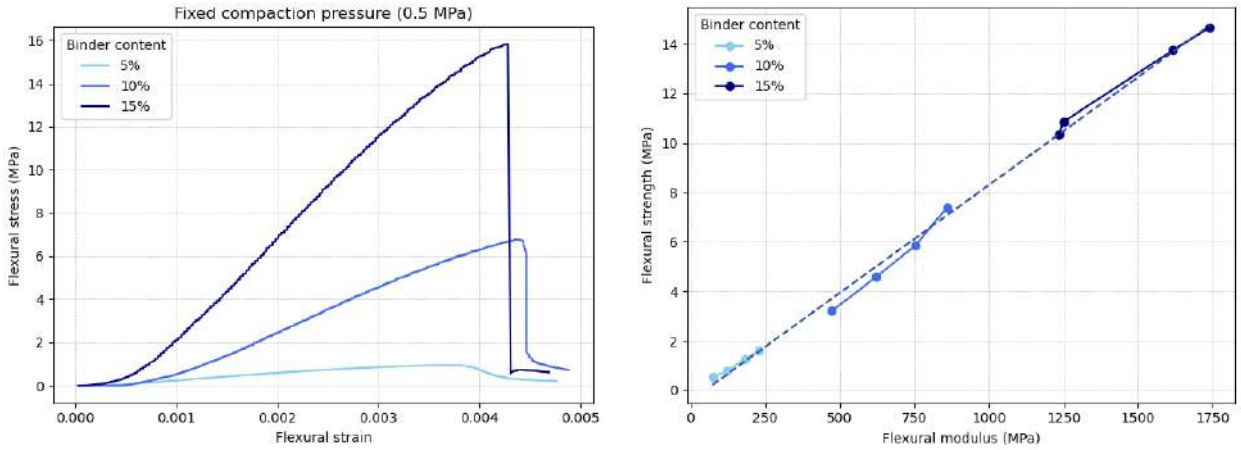

(a) (b)

Fig. 14. (a) Flexural strain-stress curves shown by the specimens for fixed compaction pressure. (b) Flexural strength vs flexural modulus.

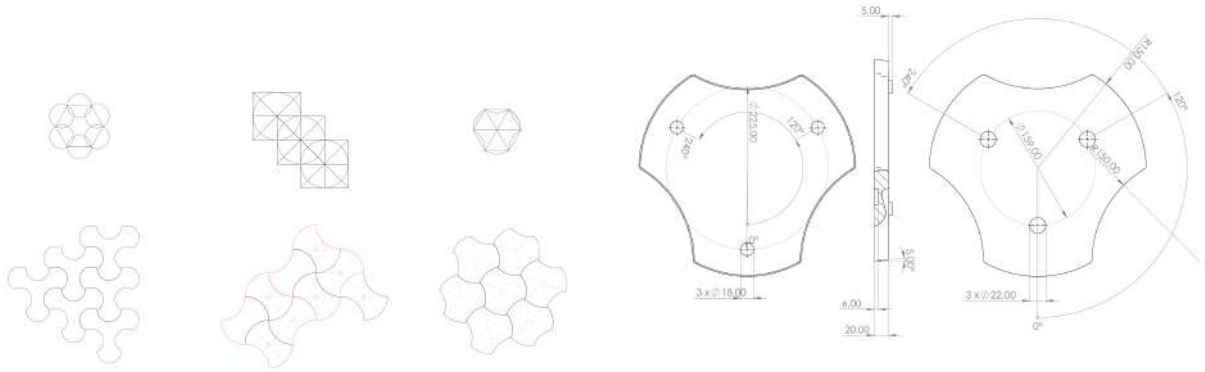

(a) (b)

Fig. 15. (a) First step in the form-finding process adopted for the design of the tile. (b) Technical drawing of the final tile design viewed from the top (left) side (center) and bottom (right). All the relevant dimensions are given in mm.

and the maximum payload is 4000 kg;

- The Descent module is provided with four hexagonal feet, each with a side of about 234 mm;
- The four feet of the lander are made of aluminum Ergal 7075 ($\rho = 2.88\ g/cm^3$, $\nu = 0.33$, $E = 71700\ MPa$)

The material properties of the regulith-PEEK mixture are taken from Fig. 14b.

4.2.1 Model

To accurately represent the complex geometry of the tiles while maintaining computational efficiency, a hybrid meshing approach was employed. Quadrilateral, HEPH-8 solid elements were used as the primary element type while to capture the curved surfaces of the tiles precisely, triangular TET elements were strategically inserted. It is assumed that the group of tiles under analysis must sustain the weight of a quarter of the lander, acting on the contact surface between the pad and one of the lander's foot. The lander's foot was simplified as a hexagonal surface, modelled with triangular shell elements, in order to keep a

low computational cost. The mass of the lander was then lumped in a single node located on the apex of a fictitious pyramid, having the hexagonal surface as base. This approach allowed for efficient calculation of the load applied to the tiles while maintaining reasonable accuracy.
The result of the meshing process is shown below (Figure 16b):

The equivalent load for each foot is applied as a vertical force on the foot's master node, calculated using the Moon's gravity, approximately $g_M \simeq 1.635\ m/s^2$. The bottom of the tile assembly is fully constrained, preventing any movement in all directions. An initial velocity is imposed on the lander, with its magnitude used as an optimization parameter to simulate the dynamic landing.

The last step for the simulation has been the choice of the material models. A key assumption of this work is to neglect the thermal gradients introduced by the impinging jets from the thrusters, thus focusing just on pure mechanical response. This was primarily due to the unavailability of thermal property data for the regolith-PEEK mixture. Future analyses will incorporate these data as they become available through ongoing testing.

The lander's foot has been modelled as a simple, infinitely elastic material. This choice was justified by the fact that the considered aluminum is between 2 and 3 orders of magnitude more resistant than the considered regulith-PEEK mixtures and thus it is fair to assume that it will remain in the region of linear elasticity.

Regarding the tiles, a first round of simulation was performed using a perfectly elastic model, exploring the allowable speed range. In order to have a better understanding of the pad's response a finer material model was used. In RADIOSS environment, the most suited candidate is the Johnson–Cook[53]. The required inputs are the following:

- Material density and ultimate strength;
- Poisson coefficient, estimated equal to 0.3, on the base of a statistical analysis of similar materials;
- Yielding strength, estimated as 5% lower than the ultimate strength. Again, this is a result of the statistical analysis;
- The engineering strain at failure estimated by approximated the stress-strain curves shown in figure 17 to right-angled triangle and thus evaluating the required strain as: $\varepsilon_{UTS} = \dfrac{\sigma_{UTS}}{E}$

4.3 Results

Reference [54] and [55] suggest that the modern optimal control theories will enable future vehicles to land on the Moon with an impact velocity in the range of 0.1 to 1 m/s, depending on their mass and propulsion system. To determine the limit velocity, a bisection method was employed. Starting with initial bounds of 0 and 1 m/s, a series of simulation were performed, comparing the maximum stress reached in the structure depicted in Figure 16b with the ultimate value bearable by the material. The velocity bounds were narrowed based on these comparisons. The process has been set to stop when reaching a precision on the final interval of 10^{-2}. This precision was deemed adequate for a preliminary model. The results of this process are listed in Table 1:

The speed limits obtained, particularly those referring to binder percentages greater than 5, already cover a fair amount of the range of landing speeds cited at the beginning of this paragraph. The data obtained for binder percentage of 5, 10 and 15, are further processed in order to extract an estimate of what properties should the material have to cover impacts up to 1 m/s.
This estimate can be achieved by considering that experimentally, the flexural strength is found to be linearly proportional to the flexural modulus and the square of the binder content ($\sigma_{f,max} \sim E_f$ and $\sqrt{\sigma_{f,max}} \sim B(\%)$). These relationships suggest that a linear relationship is also present between the square of the binder content and the *modulus of resilience*, defined as $R = \sigma^2_{f,max}/E_f$. This is experimentally verified. Considering that the modulus of resilience is related to the energy absorbed by the material before yielding [56], it can be related to the maximum impact speed through the kinetic energy as: $R \sim T = \frac{1}{2}mv^2_{max} \sim v^2_{max}$. Thus, a linear relationship between maximum impact speed and binder content is expected since $v_{max} \sim \sqrt{R} \sim B(\%)$. Remarkably, the plot in Fig. 17a proves this derivation and by considering the maximum compaction pressure, allows to predict that a binder content of 21% should allow the tile to withstand a 1 m/s landing.
The material properties for this new binder content can then be estimated through the aforementioned relationships. The self consistency of the approach followed in this work can be proven by applying again the bisective method described earlier, yields to a value of limit velocity for this new material of $v_{max} \sim 0.9\ m/s$, which is fairly close to the predicted value of 1 m/s, with the maximum stress field shown in Figure 17b.

The discrepancy between the predicted value and the actual speed could be due to both the small sample of mechanical properties that led to the linear regression employed before or the quality of the model itself that has to be refined in future iterations.

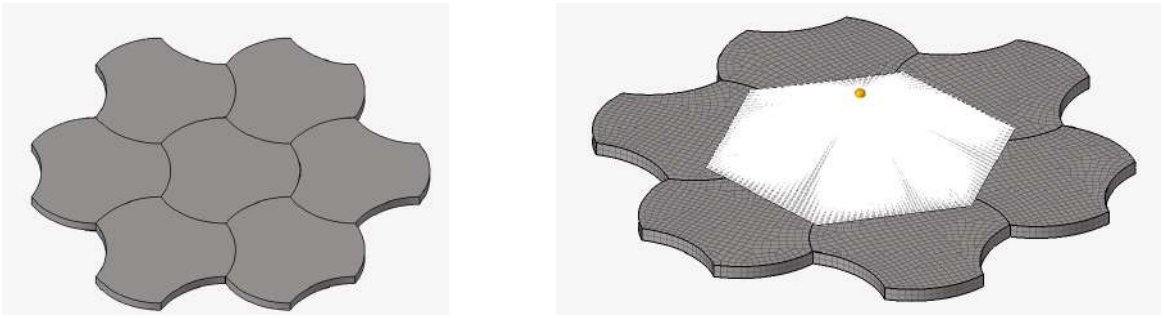

(a) (b)

Fig. 16. (a) Interlocked tiles. (b) FEM model.

DoE run no.	1	2	3	4	5	6	7	8	9	10	11	12
v_{max} $[m/s]$	0.02	0.05	0.12	0.15	0.22	0.30	0.35	0.42	0.50	0.55	0.60	0.62

Table 1. Limit speed

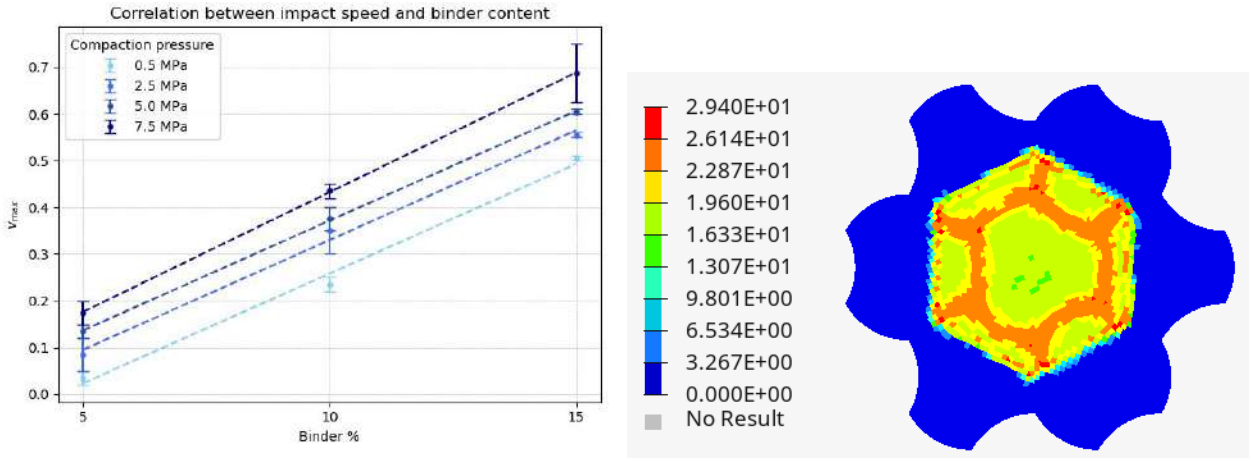

(a) (b)

Fig. 17. (a) Impact speed vs binder percentage. (b) Stress field during the impact.

5. Energy Supply

The in-situ manufacturing of regolith tiles and the provision of essential services to astronauts prescribe the availability of power sources in the lunar outpost. Designing a robust power supply system capable of withstanding the harsh lunar environment is a significant challenge to face. For this reason, this study examines two common energy production systems, namely solar arrays and nuclear fission reactors, due to their potential for reliable performance and high power output, respectively. In order to achieve meaningful results, the analysis comprises five key stages:

- Power budget formulation for a 6-human settlement on the Moon;
- Preliminary evaluation of solar and nuclear energy systems and technology selection through comparative analysis of their respective benefits and drawbacks;
- Review of the current solutions for the selected technology;
- Modeling of the chosen power system and conducting a parametric study to assess the key design parameters;
- Design optimization utilizing insights from the review on existing solutions.

These stages aim to develop an optimal power supply solution for lunar exploration, by combining the peculiar aspects of a theoretical model with practical challenges to tackle on lunar surface.

6. Power Budget Analysis

To estimate the power budget required for a 6-person lunar base, data available in the literature ([57], [58], [30], [59] and [60]) are employed. Additional estimates are derived by combining research findings with logical reasoning to obtain a comprehensive understanding of the energy demands. Firstly, the power budget of a lunar station must account for the contributions from two different types of power requirements:

- **constant power**, used to run primary circuits, ensure life support, provide communication and make sure scientific equipment works properly;
- **intermittent power**, subjected to peaks, employed for non-permanent activities, like EVA operations, rover charging and ISRU (e.g. In-Situ Resource Utilisation).

In Table 2 each segment is reported with the estimated value of power required. The higher the safety factor is, the more uncertain is the estimation of the associated activity. A safety factor of 1.2 is used only for data already present in literature, whereas higher values show huge uncertainty, which should be mitigated by further studies. A particular attention is given to ISRU activity, one of the main goals to achieve to encourage human permanence in lunar environment.
To be conservative, a total power budget of **65 kWe** is computed, resulting from the simultaneous combination of constant power and total intermittent power (safety factors included).

7. Technology analysis and selection

Given a worst case scenario in which the resulting power budget has to be really delivered, both solar arrays and nuclear fission reactors have been briefly examined, in order to make an informed decision.

7.1 Solar arrays

Although solar arrays might initially appear to be a promising option for lunar power generation, they are affected by the lunar day-night cycle, with about half of each lunar day spent in darkness. Moreover, the planned location for the Artemis missions and future lunar outposts adds another layer of complexity: at the latitude of the Shackleton crater, 89.67°S [61], illumination is a significant constraint due to the small Moon's solar angle, that is 1.5° [62]. Notably, there are permanently shadowed regions where sunlight never reaches the surface, making these areas unsuitable for solar energy production [63]. Thus, solar panels are only partially effective in meeting energy demands, requiring a massive storage system, namely made of batteries, to supply power when the panels are not receiving sunlight. Finally, employing the formulas and the typical material values from Colozza [62], as well as the power budget in Table 2, it is determined that a total mass of **66,241 kg** is required to power the settlement. The total mass accounts for only the panels and batteries, excluding wiring and other components.

7.2 Nuclear fission reactors

Nuclear fission reactors represent another viable option for energy production on the Moon, especially for their modularity and scalability characteristics, as well as their output power capabilities. Unlike solar arrays, nuclear reactors do not require batteries, as their operation is not dependent on light conditions. However, a major issue arises from the dose radiation emitted in case no shield is considered. By referring to Colozza [62], a 10 kWe nuclear reactor requires 2.82 km of distance from the habitat so as to ensure human safety, by keeping the dose below the tolerated limit of $5\ rem/y$ [64]. A total mass of $\mathbf{7,931\ kg}$ is computed to meet the power budget demands.
In the end, both the specific power delivered and the possibility to overcome the safety-related issue through an underground installation by taking advantage of the shielding properties of regolith, were paramount to opt for nuclear fission as main source of power.

8. Evaluation of Existing Nuclear Reactor Designs

Following the selection of nuclear power, it is essential to assess existing solutions to identify the most appropriate options for the project's specific needs. This evaluation involves a comprehensive review of current solutions, acknowledging that the analysis may be limited by the sensitive nature of the subject and, consequently, the scarcity of technical details in the literature.
In particular, the review focuses on three reactors - LEGO, SC-SCORE, and FSP. A brief overview of these reactors is provided, along with a comparative analysis in Table 3, which will prove to be useful to obtain a final configuration.

8.1 LEGO Reactor[65]

LEGO (Lunar Evolutionary Growth-Optimised) Reactor is a modular, fast-fission, heatpipe-cooled clustered reactor system for lunar-surface power generation. It consists of subcritical units that can be safely launched and emplaced into lunar regolith holes. Each subunit uses

POWER	ACTIVITY	VALUE	SAFETY FACTOR
Constant power	Housekeeping	5	x1.2
	Lighting	0.5	x1.2
	Life Support	16	x1.2
	Communication	1	x1.2
	Scientific equipment	2	x1.2
Total 1		24.5 kWe	29.4 kWe
Intermittent power (only peak powers are reported, to consider a worst-case scenario: all systems consume maximum power at the same time)	Crew support	17.9	x1.2
	EVA floodlights	2	x1.2
	Rover charging	3	x1.2
	ISRU activity:		
	- Scoop and delivery conveyors of raw material (regolith)	0.2	x5
	- Manufacturing of the brick (Layer deposition, Compression)	0.3	x2
	- Check on the quality	0.1	x5
	- Assembly of bricks	0.2	x5
	- Automatic system for monitoring the health status of the tool	0.5	x5
	- Automatic movement of the tool (if needed)	0.5	x5
Total 2		24.7 kWe	35.6 kWe
Total		49.2 kWe	65 kWe

Table 2. Power budget estimated for a 6-human lunar base ([57],[58],[30],[59],[60]).

uranium-dioxide fuel, stainless-steel cladding, and liquid-sodium heatpipes for heat transfer. The system employs a free-piston Stirling engine for power conversion, with a minimum five-year operational lifetime. A single unshielded subunit weighs 448 kg, provides about 5 kWe, and measures 8.77 meters in height and 0.50 meters in diameter when fully extended.

8.2 SC-SCORE Reactor[66]

SC-SCORE (Solid Core-Sectored Compact Reactor) is designed for continuous power generation in lunar outposts, providing 38 kWe for approximately 21 years. It operates at 1.0 MWth and consists of six sectors cooled by liquid NaK-56. The reactor uses highly enriched uranium nitride fuel and is emplaced in a 2.5-meter-deep trench covered with regolith for shielding and neutron reflection.

8.3 Fission Surface Power Project[67]

The Fission Surface Power Project, an expansion of the Kilopower project, aims to develop a 40 kWe Lunar Fission Surface Power Concept. It uses high-assay low-enriched uranium fuel, sodium-molybdenum heat pipes, and a yttrium hydride moderator. The reactor provides 250 kWth for 40 kWe over a 10-year lifespan. Power conversion uses eight 6.2 kWe Stirling convertors, and the system features a deployable accordion-style radiator.

9. Model of the shielded nuclear reactor plant

After providing a brief review of existing solutions, a parametric analysis based on a power plant representative model is performed to identify an optimal nuclear power system design for the lunar outpost. The attempt is to use regolith shielding effect to overcome the nuclear radiation issues for human safety, by keeping an eye to other high-level requirements as well, such as a preferable modular configuration and power consumption minimization to shield the reactors.

9.1 Model overview and main assumptions

In fig. 18, 19 and 20, three different views of the nuclear plant model developed are illustrated. The main assumptions are listed hereafter:

- The reactors use Uranium-235 fission to provide power;
- N_r is the number of reactors and they all generate the same amount of power;
- The reactors are aligned along a straight line and the spacing γ is the same for all;
- The reactors are installed in a open-vacuum hole, thus the shielding effect is ensured by the ground regolith itself surrounding the hole;
- For conservative reasons, the total radiation from a single reactor is assumed to be concentrated in the

Reactor	Pros	Cons
SC-SCORE	Compact design, lunar regolith shielding	Lower power output, limited modularity
LEGO	High modularity, ISRU alignment	Height issues
FSP	Mobile, aligns with power needs, proven components	Larger, heavier

Table 3. Pros and Cons of Reactor Designs

upper central portion of the bulk. This assumption minimizes the attenuation effect by the regolith, as the radiation travels through the least amount of matter.

- Regolith is considered totally absorbent and scattering is neglected.
- The degrees of freedom of the model are the number of reactors N_r, the coordinates of the point $P(x, y, z)$ in 3D space, the spacing γ, the hole width B and the vertical distance between the local ground level and the top of reactor bulks, called offset off.

Through some trigonometrical steps, it is possible to determine the lengths of the three segments in which a radiation ray emitted by a specific reactor can be divided: $l_n - l_{att_n}$ in vacuum, l_{att_n} into the regolith and r_{ext_n} in vacuum again (Fig. 20). As a result, either a quadratic decay model or an exponential attenuation model can be applied appropriately to compute the total dose radiation of reactor n in a certain point $P(x, y, z)$ in space. Since additivity applies here, the whole dose concentrated into that point is obtained by summing up algebraically the contributions from each reactor, leading to a 3D radiation mapping.
By referring to fig. 21, the entire process to derive the dose emitted into the space is schematized and two main aspects must be clarified: the expression for D_{1n} is obtained as a semi-empirical law correlating the minimum human safety distance with the electric power P_{el} delivered by a reactor and it relies on interpolation through data available in literature [62]; on the other hand, the coefficient k in D_{2n} is computed analytically as the product of the regolith mass attenuation coefficient μ/ρ (based on an average chemical composition [68]) equal to $0.0219\ cm^2/g$, by the regolith density ρ close to the surface [69], approximately $1.6\ g/cm^3$. In the end, $k = 0.035\ cm^{-1}$ is considered. The numbers 1,2 and 3 refer to the segment, since they indicate the amount of radiation dose at the end of each, whilst n refers to the generic reactor, among N_r reactors overall.

9.2 Parametric studies and design optimisation tips

Since the model described depends on the several degrees of freedom described, some studies have been carried out in order to detect the most impactful parameters in terms of reduction of safety distance required, by guaranteeing energy savings to dig the hole at the same time.

- 1^{st} study: the aim is determining how the offset off impacts on the minimum safety distance r_s, with P_{el}, γ and N_r fixed. It seems convenient to choose an offset from ground level within a range of $[40 - 60]$ cm: beyond this interval, the gain in r_s is almost negligible and the amount of regolith to be dug becomes too elevated with consequent increase in power consumption (fig.22). If cosmic radiation is summed up to nuclear radiation, naturally r_s increases, but the effect is not so evident.
- 2^{nd} study: the aim is assessing the effect of N_r on r_s, by keeping P_{el}, off and γ fixed. As shown in fig. 23, the effect is minimal. In fact the value of r_s ranges from 90.7 m to 93.2 m for respectively $N_r = 8$ and $N_r = 2$. It means the number of reactor is not paramount in fulfilling safety requirements, but the final decision will be taken by considering other constraints, like need of redundancy or easiness of maintenance.
- 3^{rd} study: the aim is investigating on how the inter-distance γ affects r_s. Higher values of γ, given a fixed N_r, yield better results, since r_s decreases. However, the reduction is little, thus γ is not a safety-critical parameter (fig. 24).

The definitive values for each degree of freedom of this model have to take into account technological and standardisation constraints. A reasonable compromise could be a **5** or **6-reactor** plant, with an inter-distance γ among reactors of $\mathbf{3 - 5\ m}$, a B value of **3 m** (a maximum radius of $1.5\ m$ seems acceptable by looking at the existing reactors) and a safety distance obtained around $\mathbf{r_s = 90\ m}$. Appropriate safety factors could be applied to r_s, to overcome the simplifications of the model, though they are always assumed through a conservative perspective. What really matters, however, is the overall reduction in terms of distance between settlement and plant in case of shielded plant. As a matter of fact, this approach permits to save hundreds of metres of cables and reduces energy dispersion, even by

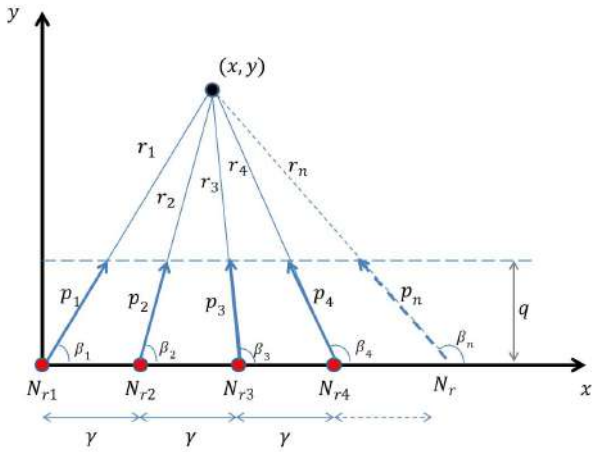

Fig. 18. View from above.

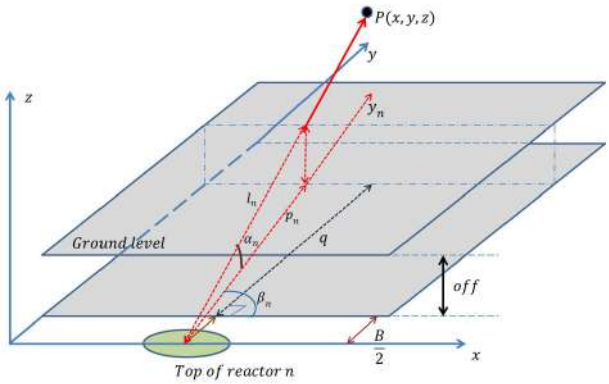

Fig. 19. View in perspective.

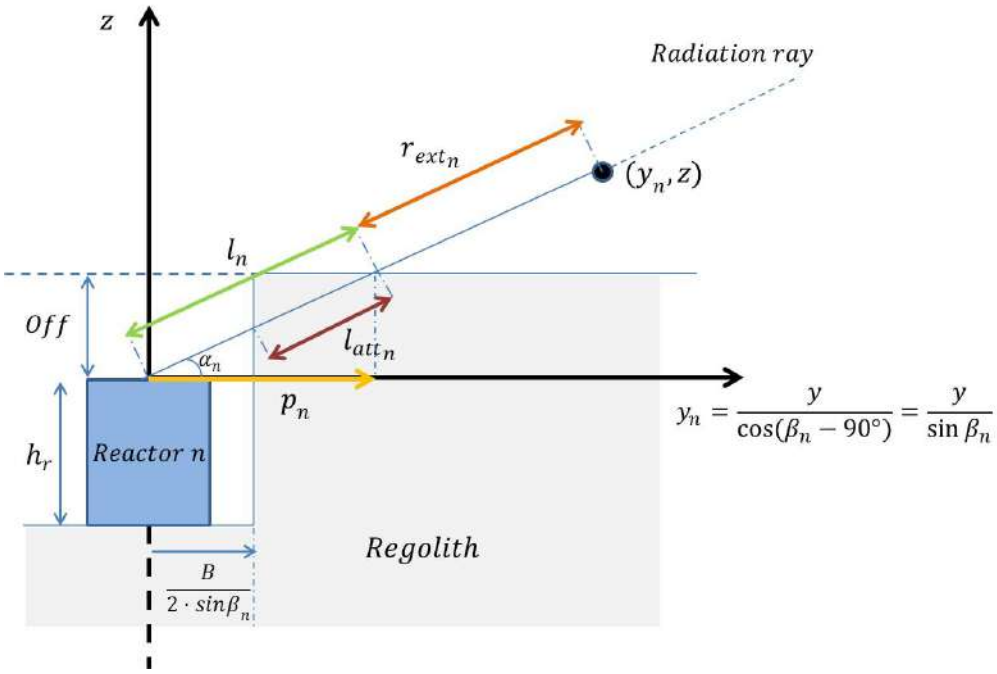

Fig. 20. View from a side.

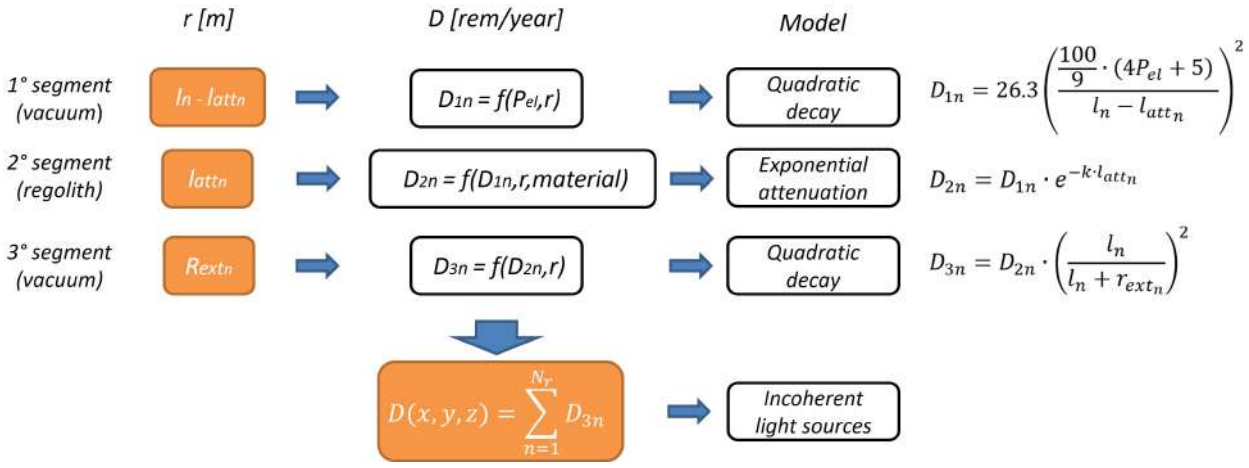

Fig. 21. Process of 3D radiation mapping.

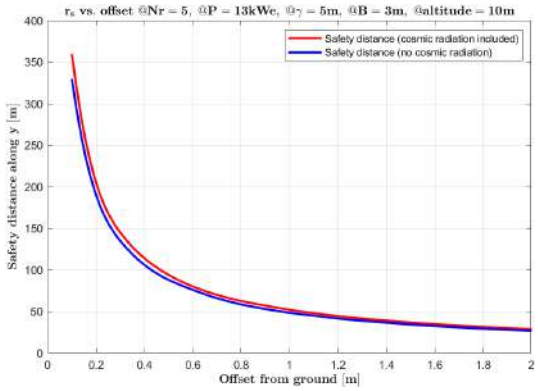

Fig. 22. Safety distance as a function of lunar ground offset, $r_s(off)$.

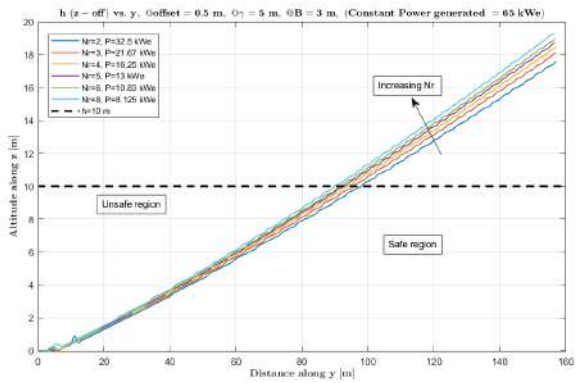

Fig. 23. Safety distance as a function of N_r, $r_s(N_r)$.

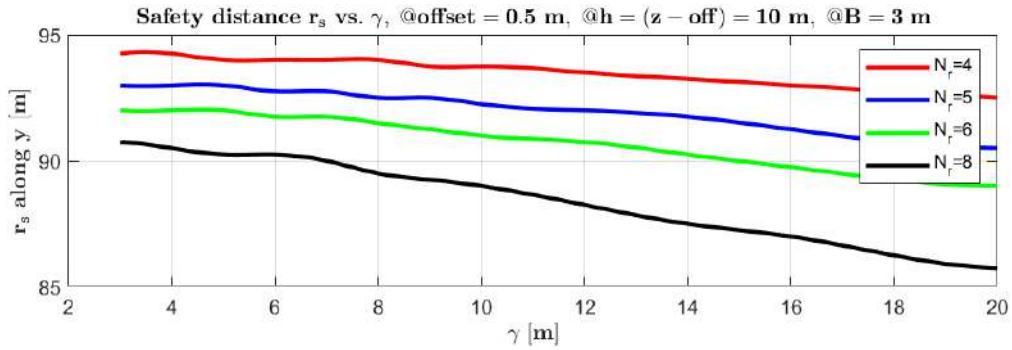

Fig. 24. Effect of γ on r_s.

applying safety factors, being still compliant with human safety limitations. If no shields were considered, 2.81 km would be necessary to protect astronauts from the radiation dose of a 6-reactor plant of 60 kWe overall [62], making the project impracticable due to the distance with the settlement.
Finally, in fig.25, a generic graphical outcome of the model is reported: the reactors, the regolith and the the iso-dose radiation surfaces,(the lower one accounts for cosmic radiation) are included to discern easily from safe and unsafe regions.

10. Final Design

A comprehensive set of evaluation parameters, including mass, power output, size, modularity, and ISRU compatibility, has been established to facilitate a rigorous comparison of the reactor options illustrated in the review, to decide which configuration best fit in the theoretical model presented.
The FSP reactor emerges as a leading candidate, particularly due to its alignment with the MOSS project's power requirements and human capacity needs. Its configuration, consisting of six reactors providing a total power output of 40 kWe, closely matches the project's specifications. However, the FSP reactor is designed for installation directly on the lunar surface, which introduces significant challenges concerning its distance from the habitat and compliance with safety protocols.
Among the alternative options, the SC-SCORE reactor shows promise due to its compactness, both in diameter and in height, which minimizes excavation requirements, thus the energy expenditure needed.
Furthermore, LEGO reactor's modularity and use of regolith as a reflector present additional design advantages that could be beneficial if integrated into the final solution.
The optimal reactor design for the MOSS project would incorporate the power output, reactor configuration, and diameter of FSP reactor, the compactness of SC-SCORE reactor, and the modularity of LEGO reactor. This hybrid approach would best satisfy the comprehensive requirements of the MOSS project, ensuring a balance between power generation, operational efficiency and safety considerations.

11. Conclusions and Future Work

This project explored the design of a Lunar Outpost using an integrated approach aimed at delivering a holistic solution. Specifically, the study focused on three key areas: Architecture, Materials, and Energy, each of which is interconnected with the others.
The study began by identifying the optimal location for the outpost at the South Pole of the Moon. This involved analyzing lunar geology using data from various lunar missions, leading to the selection of Shackleton Crater due to its significant ice deposits. To inform the design process, the project reviewed existing spaceport and architectural precedents, drawing inspiration from concepts such as airports, movie sets, and lunar infrastructures. Following the completion of the lunar infrastructure study and site selection, a temporal dimension was introduced. This involved developing three distinct design scenarios for the future outpost, categorized into phases based on the base's population level. For the medium-term scenario, the project envisioned the base in Shackleton Crater, consistently inhabited by four/six astronauts. This also motivated the identification of the needs of the astronauts.

Following this study, the choice was made to concentrate on the lunar landing pad infrastructure. The design of the landing pads and supporting infrastructure was informed by terrestrial analogs such as Spaceport America and Project Olympus, with modifications to account for the lunar environment, including the containment of dust and debris through protection walls. At this point, the focus shifted to the design and validation, through numerical simulations, of a structural element crafted from a material optimized for ISRU. In particular, the core element of the study is a tile designed to withstand the landing of the European Large Logistic Lander. The design process began with an in-depth study of the properties of the chosen material: a PEEK-regolith blend. Stress-strain curves derived from flexural testing revealed a brittle behavior, with the specimens showing very limited plasticity. Despite this, the specimens demonstrated good resistance even with a low binder content. The specifics of the production process associated with the composite material dictated the design of the tile, which was chosen to have hexagonal symmetry in order to maximize resistance and minimize potential production defects. The design was validated through finite element analysis, where the maximum landing speed was determined as a function of binder content for each compaction pressure used in material testing. A linear trend was observed, which could, in principle, allow future researchers to estimate the safe landing speed for binder contents other than the three values for which mechanical properties were known. This observation was rationalized by considering that the maximum impact speed could be related, through the maximum kinetic energy, to the modulus of resilience, which exhibited a linear trend with the square of the binder content. The fact that the modulus of resilience followed this trend was further explained by noting that the flexural strength and modulus were linearly dependent on each other, and that the square root of the strength was linearly proportional to the binder content. To demonstrate the self-consistency of these findings, the lin-

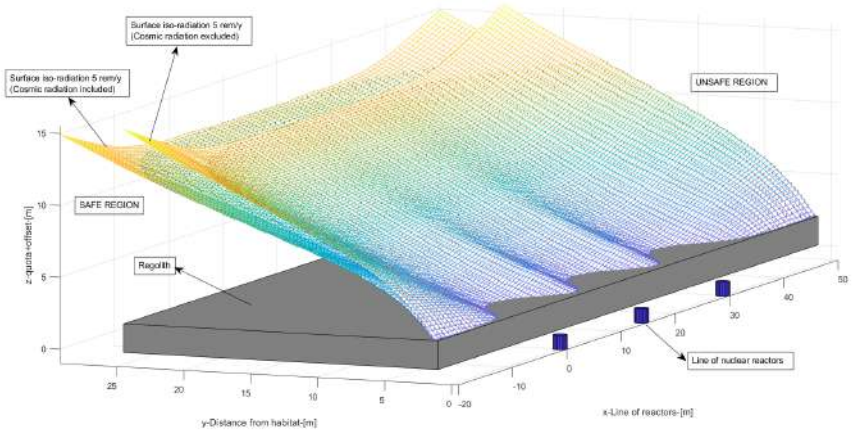

Fig. 25. Surfaces iso-radiation resulting from the model.

ear relationships were used to estimate the binder content required to withstand an impact at 1 m/s. Extrapolating the material properties, the maximum impact speed that could be withstood by a tile with 21 wt. % binder was evaluated at 0.9 m/s, which is close to the predicted value of 1 m/s.
At this stage, given the power demands for sustaining astronaut and producing tiles, it became essential to explore potential power supply solutions. The study began with an analysis of the power budget required to support a lunar outpost, considering both the energy needed for a stable habitat for six astronauts and the production of tiles for the landing pad.
To supply the required power, a preliminary assessment of solar panels and nuclear fission reactors was conducted. Given that the outpost location is poorly illuminated and the significant mass of a solar panels power plant, nuclear fission emerged as the sole viable energy solution. Consequently, the focus shifted to identifying the optimal configuration for supplying energy to the lunar base while ensuring adequate radiation shielding. A parametric study evaluated factors such as safety distance from the base, number of reactors, inter-reactor spacing, and physical dimensions. The analysis revealed that none of the existing reactor designs fully meet the optimal conditions. For instance, increasing the number of reactors from 4 to 8 reduced the required safety distance only slightly, from 94 m to 89.7 m. Similarly, increasing the inter-reactor distance from 3 m to 20 m resulted in just a 5 m reduction in safety distance, making this factor less critical. However, a combination of features from various designs emerged as a promising solution. A configuration with 5 or 6 reactors, spaced 3 to 5 m apart, provided a safety distance of around 90 m while minimizing excavation energy requirements. This setup balances radiation protection and operational efficiency, with manageable excavation costs as the energy required scales linearly with the volume of regolith removed. Although no single design perfectly matches the optimal requirements, this hybrid approach leverages the advantages of modularity and redundancy from smaller reactors, along with compact design features from larger reactors, to achieve an effective energy supply system for the lunar base.

Given to the holistic approach of the Project MOSS, future works should aim to further investigate the explored areas and explore new sectors and their interconnections, building on the project's foundation. This includes refining the technical details of ISRU and 3D printing technologies, optimizing the placement of infrastructure, and addressing the challenges of long-term habitation. While Phase 3, a fully autonomous lunar colony, remains beyond the current scope, the foundations laid by this study provide a roadmap for future lunar exploration and settlement. Further testing is necessary to validate the reliability of the findings related to tile production. This includes full-scale assessments of the tile design to evaluate its resistance to booster rocket firing during takeoff, as well as its durability under the harsh temperatures and radiation on the lunar surface. Additionally, while not considered here, fission reactors designed for terrestrial applications could be studied for potential adaptation to the lunar surface. Future work should also refine parametric studies to explore alternative reactor configurations, which could bring reactors closer to the outpost, reduce wiring needs, facilitate supply logistics while preserving base safety.

References

[1] F. Gramazio, M. Kohler, and S. Langenberg, *Fabricate 2014: Negotiating Design & Making*, en. UCL Press, Aug. 2017, ISBN: 978-1-78735-214-8. DOI: 10.2307/j.ctt1tp3c5w. [Online]. Available: http://www.jstor.org/stable/10.2307/j.ctt1tp3c5w (visited on 09/03/2024).

[2] P. Gruber, S. Häuplik, B. Imhof, K. Özdemir, R. Waclavicek, and M. A. Perino, "Deployable structures for a human lunar base," en, *Acta Astronautica*, vol. 61, no. 1-6, pp. 484–495, Jun. 2007, ISSN: 00945765. DOI: 10.1016/j.actaastro.2007.01.055. [Online]. Available: https://linkinghub.elsevier.com/retrieve/pii/S0094576507000690 (visited on 09/03/2024).

[3] The Free Dictionary, *Selenodesy*, https://www.thefreedictionary.com/selenodesy, [Online; accessed 2024-09-11].

[4] NASA Science, *Lunar Reconnaissance Orbiter - NASA Science*, en-US, https://science.nasa.gov/mission/lro/, [Online; accessed 2024-09-11].

[5] Lunar and Planetary Institute (LPI), *Unified Geologic Map of the Moon*, en, http://www.lpi.usra.edu/resources/mapcatalog/UGM/, [Online; accessed 2024-09-11].

[6] Lunar and Planetary Institute (LPI), *Lunar South Pole Atlas*, en, https://www.lpi.usra.edu/lunar/lunar-south-pole-atlas/, [Online; accessed 2024-09-11].

[7] Maps on the Web, *Geologic map of the south side of the moon*, Tumblr, Available at: https://mapsontheweb.tumblr.com/post/169964060986, Accessed: 2023-09-19, 2023.

[8] Lunar and Planetary Institute (LPI), *USGS Shaded Relief Maps of the Moon - I-1326A*, en, http://www.lpi.usra.edu/resources/mapcatalog/usgsTopo/I1326A/, [Online; accessed 2024-09-11].

[9] E. Gough, *A Geologic Map of the Entire Moon has Been Released at 1:2,500,000-Scale*, en-US, https://www.universetoday.com/156265/a-geologic-map-of-the-entire-moon-has-been-released-at-12500000-scale/, [Online; accessed 2024-09-11], Jun. 2022.

[10] Lunar and Planetary Institute (LPI), *150dpi.jpg (2400×1647)*, https://www.lpi.usra.edu/resources/mapcatalog/LC1/images/150dpi.jpg, [Online; accessed 2024-09-11].

[11] Lunar and Planetary Institute (LPI), *Lunar Chart (LPC-1)*, en, http://www.lpi.usra.edu/resources/mapcatalog/LC1/, [Online; accessed 2024-09-11].

[12] Spaceport America, *Home*, https://spaceportamerica.com, [Online; accessed 2024-09-11].

[13] Space Port Japan, *Space Port Japan*, ja, https://www.spaceport-japan.org, [Online; accessed 2024-09-11].

[14] E. Howell, *Spaceport America: Space Tourism Launch Site*, en, https://www.space.com/19258-spaceport-america.html, [Online; accessed 2024-09-11], Aug. 2019.

[15] daa International, *Red Sea International Airport*, en-US, https://www.daa-international.com/airports/international-airports/red-sea-airport/, [Online; accessed 2024-09-11].

[16] Evostel, *Evostel - Experts in IoT, Automation and Energy Solutions*, en, https://www.evostel.com/projects/amaala, [Online; accessed 2024-09-11].

[17] Britannica, *France | History, Maps, Flag, Population, Cities, Capital, & Facts | Britannica*, en, https://www.britannica.com/topic/Terminal-1-at-Paris-Charles-de-Gaulle-Airport, [Online; accessed 2024-09-11], Aug. 2024.

[18] 2001: A Space Odyssey Wiki, *Clavius Base*, en, https://2001.fandom.com/wiki/Clavius_Base, [Online; accessed 2024-09-11].

[19] Independence Day Wiki, *Rhea Base*, en, https://independenceday.fandom.com/wiki/Rhea_Base, [Online; accessed 2024-09-11].

[20] Paolo Giandoso, *Paolo Giandoso - Independence Day: Resurgence, Destruction of Rhea*, https://paologiandoso.artstation.com/projects/dEokX?album_id=989352, [Online; accessed 2024-09-11].

[21] Dezeen, *BIG and NASA collaborate to design 3D-printed buildings for the moon*, en, https://www.dezeen.com/2020/10/01/project-olympus-big-icon-nasa-moon-buildings-3d-printed/, [Online; accessed 2024-09-11], Oct. 2020.

[22] SpaceX, *SpaceX - Missions: Moon*, https://www.spacex.com/humanspaceflight/moon/, [Online; accessed 2024-09-11].

[23] Foster + Partners, *Mars Habitat | Architecture Projects*, en, https://www.fosterandpartners.com/projects/mars-habitat, [Online; accessed 2024-09-11].

[24] P. Schmid, "Lunar far-side communication satellites," National Aeronautics and Space Administration, Washington, D.C, Springfield, Va., Tech. Rep., 1968, For sale by the Clearinghouse for Federal Scientific and Technical Information.

[25] C. Burke and R. Howard, "Internal layout assessment of a lunar surface habitat," *ASCEND 2022*, 2022, [Preprint]. DOI: 10.2514/6.2022-4266.

[26] C. Stromgren et al., "Defining the required net habitable volume for long-duration exploration missions," *ASCEND 2020*, 2020, [Preprint]. DOI: 10.2514/6.2020-4032.

[27] J. Wertz and W. Larson, *Space mission analysis and design*. Torrance, Calif; Dordrecht, The Netherlands: Microcosm Press; Kluwer Academic, 1999.

[28] A. Colozza et al., "Solar energy systems for lunar oxygen generation," *48th AIAA Aerospace Sciences Meeting Including the New Horizons Forum and Aerospace Exposition*, 2010, [Preprint]. DOI: 10.2514/6.2010-1166.

[29] Jingsun New Energy And Technology Co.,Ltd., *From earth to the moon: Analyzing the performance of solar panels in space - knowledge*, 2023. [Online]. Available: https://www.jingsun-power.com/info/from-earth-to-the-moon-analyzing-the-performa-88740902.html.

[30] C. Molteni, "Preliminary architecture of nuclear space reactor for a lunar base," thesis, Politecnico di Milano, 2022.

[31] M. Gibson et al., "Nasa's kilopower reactor development and the path to higher power missions," in *2017 IEEE Aerospace Conference*, [Preprint], 2017. DOI: 10.1109/aero.2017.7943946.

[32] M. Gibson, S. Oleson, D. Poston, and P. Mcclure, "Nasa's kilopower reactor development and the path to higher power missions," in *2017 IEEE Aerospace Conference*, Mar. 2017, pp. 1–14. DOI: 10.1109/AERO.2017.7943946.

[33] M. Yashar, *Lunar landing pad designs; icon / nasa's project olympus*, No date. [Online]. Available: https://www.melodieyashar.com/lunar-landing-pad.

[34] *Elon musk's spacex returns to flight and pulls off dramatic, historic landing*, 2017. [Online]. Available: https://www.washingtonpost.com/news/the-switch/wp/2015/12/21/elon-musks-spacex-pulls-off-dramatic-historic-landing/.

[35] *Spacex landing zones*, 2024. [Online]. Available: https://maps.app.goo.gl/umq3N7GbD3hob7McA.

[36] "Spaceport design on the moon: From first launch to the future," 2020, [Preprint]. DOI: 10.2514/6.2020-4189.vid.

[37] B. Burns, "Technical paper: Lunar in-situ landing/launch environment (lill-e) pad," Report, 2021.

[38] *The apollo lunar roving vehicle*, 2016. [Online]. Available: https://nssdc.gsfc.nasa.gov/planetary/lunar/apollo_lrv.html.

[39] *Space exploration vehicle fact sheet*, 2010. [Online]. Available: https://www.nasa.gov/pdf/464826main_SEV_FactSheet_508.pdf.

[40] *Lockheed martin, general motors team-up to develop next-generation lunar rover for nasa artemis astronauts to explore the moon*, 2024. [Online]. Available: https://news.gm.com/newsroom.detail.html/Pages/news/us/en/2021/may/0526-lockheed.html.

[41] *The space shuttle and its operations*, 2023. [Online]. Available: https://www.nasa.gov/wp-content/uploads/2023/04/wings-ch3a-pgs53-73.pdf.

[42] R. Orloff, *Apollo by the Numbers*. National Aeronautics and Space Administration, 1996, p. 22, PDF.

[43] T. Russomano, "Life support systems for manned mars missions, overview," in *Handbook of Life Support Systems for Spacecraft and Extraterrestrial Habitats*, A. Unknown, Ed., Springer, 2016, pp. 1–12. DOI: 10.1007/978-3-319-09575-2_188-1.

[44] M. Rahman and S. Rahman, *Food properties handbook*. Boca Raton: CRC Press, 2009.

[45] ESA, *Cupola*, 2024. [Online]. Available: https://www.esa.int/Science_Exploration/Human_and_Robotic_Exploration/Node-3_Cupola/Cupola.

[46] B. Khoshnevis, A. Carlson, and M. Thangavelu, "ISRU-BASED ROBOTIC CONSTRUCTION TECHNOLOGIES FOR LUNAR AND MARTIAN INFRASTRUCTURES," en,

[47] K. W. Farries, P. Visintin, S. T. Smith, and P. van Eyk, "Sintered or melted regolith for lunar construction: State-of-the-art review and future research directions," *Construction and Building Materials*, vol. 296, p. 123 627, 2021, ISSN: 0950-0618. DOI: https://doi.org/10.1016/j.conbuildmat.2021.123627. [Online]. Available: https://www.sciencedirect.com/science/article/pii/S0950061821013878.

[48] C. G. Ferro, R. Torre, G. Charruaz, A. E. M. Casini, and A. Cowley, "Innovative design and construction methodologies for in-situ manufacturing of large sensorized structures in future human habitat on the moon," in *Proceedings of the 74th International Astronautical Congress (IAC)*, IAC-23.C2.9.x78443, Politecnico di Torino, German Aerospace Centre (DLR), European Space Agency (ESA), Baku, Azerbaijan: International Astronautical Federation (IAF), 2023.

[49] R. Torre, A. Cowley, and C. G. Ferro, "Low binder content bricks: A regolith-based solution for sustainable surface construction on the moon," eng, *SN applied sciences*, vol. 6, no. 3, pp. 88–, 2024, ISSN: 2523-3963.

[50] G. Cesaretti, E. Dini, X. De Kestelier, V. Colla, and L. Pambaguian, "Building components for an outpost on the lunar soil by means of a novel 3d printing technology," *Acta Astronautica*, vol. 93, pp. 430–450, 2014, ISSN: 0094-5765. DOI: https://doi.org/10.1016/j.actaastro.2013.07.034. [Online]. Available: https://www.sciencedirect.com/science/article/pii/S0094576513002889.

[51] ASTM International, *Standard Test Methods for Flexural Properties of Unreinforced and Reinforced Plastics and Electrical Insulating Materials*, ASTM Standard D790-17, West Conshohocken, PA: ASTM International, 2017. DOI: https://doi.org/10.1520/D0790-17.

[52] ESA, *Argonaut*, https://www.esa.int/Science_Exploration/Human_and_Robotic_Exploration/Exploration/Argonaut, [Online; accessed 2024-08-13].

[53] X. Wang and J. Shi, "Validation of johnson-cook plasticity and damage model using impact experiment," *International Journal of Impact Engineering*, vol. 60, pp. 67–75, 2013, ISSN: 0734-743X. DOI: https://doi.org/10.1016/j.ijimpeng.2013.04.010. [Online]. Available: https://www.sciencedirect.com/science/article/pii/S0734743X13000948.

[54] X.-L. Liu, G.-R. Duan, and K.-L. Teo, "Optimal soft landing control for moon lander," *Automatica*, vol. 44, no. 4, pp. 1097–1103, 2008, ISSN: 0005-1098. DOI: https://doi.org/10.1016/j.automatica.2007.08.021. [Online]. Available: https://www.sciencedirect.com/science/article/pii/S0005109807004025.

[55] F. Capolupo and A. Rinalducci, "Descent & Landing Trajectory and Guidance Algorithms with Divert Capabilities for Moon Landing," en, in *AIAA SCITECH 2024 Forum*, Orlando, FL: American Institute of Aeronautics and Astronautics, Jan. 2024, ISBN: 978-1-62410-711-5. DOI: 10.2514/6.2024-0086. [Online]. Available: https://arc.aiaa.org/doi/10.2514/6.2024-0086 (visited on 08/27/2024).

[56] P. Wu and T. Wu, "Temperature-dependent modulus of resilience in metallic solids – calculated from strain-electron-phonon interactions," *Journal of Alloys and Compounds*, vol. 705, pp. 269–272, 2017, ISSN: 0925-8388. DOI: https://doi.org/10.1016/j.jallcom.2017.02.150. [Online]. Available: https://www.sciencedirect.com/science/article/pii/S0925838817305881.

[57] W. J. Larson and L. K. Pranke, *Human spaceflight: mission analysis and design*. McGraw-Hill College, 1999.

[58] H. Jones, "Power management for space advanced life support," 2002.

[59] A. Haridas, "Structural health monitoring (shm) goes to space," 2021.

[60] M. Kaczmarzyk and M. Musiał, "Parametric study of a lunar base power systems," *Energies*, vol. 14, no. 4, 2021, ISSN: 1996-1073. DOI: 10.3390/en14041141. [Online]. Available: https://www.mdpi.com/1996-1073/14/4/1141.

[61] I. A. U. (W. G. for Planetary System Nomenclature, *Shackleton*, Planetary Names: Gazetteer of Planetary Nomenclature, https://planetarynames.wr.usgs.gov/Feature/5450, 2024.

[62] A. J. Colozza, "Small lunar base camp and in situ resource utilization oxygen production facility power system comparison," 2020.

[63] A. K. Ross, S. Ruppert, P. Gläser, and M. Elvis, "Preliminary quantification of the available solar power near the lunar south pole," *Acta Astronautica*, vol. 211, pp. 616–630, 2023, ISSN: 0094-5765. DOI: https://doi.org/10.1016/j.actaastro.2023.06.040.

[64] M. Wall, "We now know exactly how much radiation astronauts will face on the moon," *Space.com*, 2020.

[65] J. Bess, "A basic lego reactor design for the provision of lunar surface power," *International Conference on Advances in Nuclear Power Plants, ICAPP 2008*, Jul. 2008.

[66] T. Schriener and M. El-Genk, "Safety analysis of solid core-sectored compact reactor (sc-score)," *International Congress on Advances in Nuclear Power Plants, ICAPP 2014*, vol. 3, pp. 1714–1724, Jan. 2014.

[67] S. Oleson *et al.*, "A deployable 40 kwe lunar fission surface power concept," in *NASA Technical Reports Server (NTRS)*, Jan. 2022, pp. 519–527. DOI: 10.13182/NETS22-38629.

[68] B. M. F. Grant H. Heiken David T. Vaniman, *Lunar Sourcebook*. Cambridge University Press, 1991.

[69] "Https://www.nist.gov/pml/x-ray-mass-attenuation-coefficients," *NIST*, 2004.